

การวิเคราะห์ทางไฟฟ้าของสารประกอบที่มีซัลเฟอร์โดยใช้ฟิล์มบางของโบรอน-ไดโปกไดมอนด์  
ประยุกต์ใช้กับโพลีเอเธน



นางสาวณภัททิพย์ อักษรนันท์

สถาบันวิทยบริการ

จุฬาลงกรณ์มหาวิทยาลัย

วิทยานิพนธ์นี้เป็นส่วนหนึ่งของการศึกษาตามหลักสูตรปริญญาวิทยาศาสตรมหาบัณฑิต

สาขาวิชาเคมี ภาควิชาเคมี

คณะวิทยาศาสตร์ จุฬาลงกรณ์มหาวิทยาลัย

ปีการศึกษา 2543

ISBN 974-13-1366-7

ลิขสิทธิ์ของจุฬาลงกรณ์มหาวิทยาลัย

ELECTROANALYSIS OF SULFUR-CONTAINING COMPOUNDS USING  
A BORON-DOPED DIAMOND THIN-FILM APPLIED TO FLOW INJECTION

Miss Pakatip Aksharanandana

สถาบันวิทยบริการ

A Thesis Submitted in Partial Fulfillment of the Requirements  
for the Degree of Master of Science in Chemistry

Department of Chemistry

Faculty of Science

Chulalongkorn University


Academic Year 2000

ISBN 974-13-1366-7

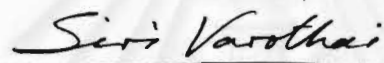
|                |  |
|----------------|--|
| Thesis Title   | Electroanalysis of Sulfur-Containing Compounds Using A Boron-Doped Diamond thin-film Applied to Flow Injection |
| By             | Miss Pakatip Aksharanandana  |
| Field of Study | Chemistry  |
| Thesis Advisor | Orawon Chailapakul, Ph.D.  |


---

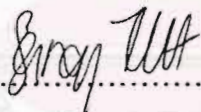
Accepted by the Faculty of Science, Chulalongkorn University in Partial Fulfillment of the Requirement for the Master's Degree

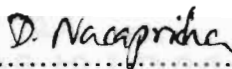
  
..... Dean of Faculty of Science  
(Associate Professor Wanchai Phothiphichitr, Ph.D.)

Thesis Committee

  
..... Chairman  
(Associate Professor Siri Varothai, Ph.D.)

  
..... Thesis Advisor  
(Orawon Chailapakul, Ph.D.)

  
..... Member  
(Sanong Ekasit, Ph.D.)

  
..... Member  
(Duangjai Nacapricha, Ph.D.)

ผกาทิพย์ อักษรนันท์ : การวิเคราะห์ทางไฟฟ้าของสารประกอบที่มีซัลเฟอร์โดยใช้ฟิล์มบางของ  
โบรอน-โดปไดมอนด์ ประยุกต์ใช้กับโพลีเอคเซน (ELECTROANALYSIS OF SULFUR-  
CONTAINING COMPOUNDS USING A BORON-DOPED DIAMOND THIN-FILM APPLIED TO FLOW  
INJECTION) อาจารย์ที่ปรึกษา : อ.ดร. อรวรรณ ชัยลภากุล; 72 หน้า. ISBN 974-13-1366-7

ออกซิเดชันของสารประกอบที่มีซัลเฟอร์เช่น cysteine, homocysteine, glutathione,  
2-mercaptoethane sulfonic acid และ cephalexin สามารถตรวจสอบได้ในตัวกลางที่เป็นบัฟเฟอร์  
ของคาร์บอเนต โดยเทคนิคไซคลิกโวลแทมเมตรี ในงานวิจัยนี้ใช้ฟิล์มบางของโบรอน-โดปไดมอนด์  
เป็นขั้วไฟฟ้าทำงานเทียบกับขั้วไฟฟ้ากลาสซีคาร์บอน ใช้ขั้วไฟฟ้าซิลเวอร์/ซิลเวอร์คลอไรด์เป็นขั้วไฟ  
ฟ้าอ้างอิง และใช้ลวดแพลทินัมเป็นขั้วไฟฟ้าเคอร์เตอร์ ผลการทดลองบ่งชี้ว่า การใช้ฟิล์มบางของ  
โบรอน-โดปไดมอนด์เป็นขั้วไฟฟ้าสำหรับตรวจวัดได้ดี มีช่วงความเข้มข้นที่ตรวจวัดได้คือ  
0.5 มิลลิโมลาร์ ถึง 10 มิลลิโมลาร์ และความเข้มข้นต่ำสุดที่ตรวจวัดได้เป็น 0.5 มิลลิโมลาร์ ยกเว้น  
cephalexin ซึ่งมีช่วงความเข้มข้นที่ตรวจวัดได้คือ 10 มิลลิโมลาร์ ถึง 25 มิลลิโมลาร์ และความเข้มข้น  
ต่ำสุดที่ตรวจวัดได้เป็น 10 มิลลิโมลาร์ อย่างไรก็ตามพบว่าผลิตภัณฑ์จากการเกิดออกซิเดชันจะปกคลุม  
ที่ผิวของขั้วไฟฟ้าและลดสัญญาณในการตรวจวัดครั้งต่อไป แต่ฟิล์มของผลิตภัณฑ์นี้สามารถกำจัด  
ออกไปได้ เราจึงเลือกโพลีเอคเซนในการแก้ปัญหา โดยระบบ FIA และฟิล์มบางของโบรอน-โดป  
ไดมอนด์ ซึ่งให้ผลการทดลองที่สามารถทำซ้ำได้ มีช่วงความเข้มข้นที่ตรวจวัดได้คือ 50 นาโนโมลาร์  
ถึง 10 ไมโครโมลาร์ และความเข้มข้นต่ำสุดที่ตรวจวัดได้เป็น 50 นาโนโมลาร์ ที่อัตราส่วนระหว่าง  
สัญญาณต่อสัญญาณรบกวนเท่ากับ 3 และสำหรับโพลีเอคเซนที่สร้างขึ้นใช้เองนั้นก็ให้ผลในการทำซ้ำที่  
ดีเช่นกัน แต่โพลีเอคเซนที่สร้างขึ้นนี้ก็มีสัญญาณรบกวนบ้าง พบว่าความเข้มข้นต่ำสุดที่ตรวจวัดได้  
ของ 2-mercaptoethane sulfonic โดยใช้โพลีเอคเซนที่สร้างขึ้นใช้เองนี้ในการวิเคราะห์อยู่ที่  
500 นาโนโมลาร์

สถาบันวิทยบริการ  
จุฬาลงกรณ์มหาวิทยาลัย

ภาควิชา.....เคมี.....ลายมือชื่อ.....  
สาขาวิชา.....เคมี.....ลายมือชื่ออาจารย์ที่ปรึกษา.....  
ปีการศึกษา.....2543.....

# # 4172367423 : MAJOR ANALYTICAL CHEMISTRY

KEY WORDS : BORON-DOPED DIAMOND THIN-FILM/ SULFUR-CONTAINING COMPOUNDS/ FLOW INJECTION ANALYSIS

PAKATIP AKSHARANANDANA : ELECTROANALYSIS OF SULFUR-CONTAINING COMPOUNDS USING A BORON-DOPED DIAMOND THIN-FILM APPLIED TO FLOW INJECTION. THESIS ADVISOR : ORAWON CHAILAPAKUL, Ph.D. 72 pp., ISBN 974-13-1366-7

The oxidation of sulfur-containing compounds such as cysteine, homocysteine, glutathione, 2-mercaptoethane sulfonic acid and cephalixin, in carbonate buffer, pH 9.2, was investigated using cyclic voltammetry. A boron-doped diamond thin-film was used as the working electrode compared with a glassy carbon electrode. Ag/AgCl electrode was employed as the reference electrode and a platinum wire was used as the counter electrode. The results indicated that a boron-doped diamond was an excellent electrode for detecting sulfur-containing compounds. A peak shape of cyclic voltammogram that received from boron-doped diamond thin-film was well-defined compared to the one from a glassy carbon electrode. A linear dynamic range of 0.5 mM to 10 mM and a detection limit of 0.5 mM were observed except cephalixin, which had a linear dynamic range of 10 mM to 25 mM and a detection limit of 10 mM. The boron-doped diamond thin-films exhibited higher sensitivity than the glassy carbon electrode. However, the oxidative products could cover the surface of electrode and decreased the next scan signal. Flow injection analysis (FIA) was chosen to overcome this problem. FIA with the boron-doped diamond thin-film electrodes provided the reproducible results. A linear dynamic range of cysteine and 2-mercaptoethane sulfonic acid was of 50 nM to 10  $\mu$ M, and the detection limit of 50.0 nM at a S/N = 3 was obtained at the boron-doped diamond thin-film. It was found that signals from a home-made flow cell were reproducible with some noises. The detection limit of 2-mercaptoethane sulfonic acid using this cell was 500 nM.

Department.....Chemistry.....Student's signature.....

Field of study.....Chemistry.....Advisor's signature.....

Academic year.....2000.....

## ACKNOWLEDGEMENT

The author would like to express her sincere to all staffs of the department of chemistry, Chulalongkorn University and teachers especially Dr. Orawon Chailapakul, great and kind advisor. She also appreciates Associate Professor Dr. Thawatchai Tuntulani for his ever-willing encouragement, Dr. Roderick Bate for his edition, Dr. Duangjai Nacapricha and Assoc. Professor Dr. Prapin Wirairat for provision equipment and suggestion, Professor Akira Fujishima for all of diamond thin-films, and Mr. Chiaki Terachima for the BAS flow cell.

She would like to thank Chulalongkorn University for financial support and atmosphere and she appreciates the supports from the development and promotion of science and technology talent project.

Lastly, she deeply appreciates and thanks her family, her closed friends and special someone for their supports.

สถาบันวิทยบริการ  
จุฬาลงกรณ์มหาวิทยาลัย

# CONTENTS

|   | Page |
|---|------|
| <b>ABSTRACT (in English)</b> .....  | iv   |
| <b>ABSTRACT (in Thai)</b> .....   | v    |
| <b>ACKNOWLEDGEMENT</b> .....  | vi   |
| <b>CONTENTS</b> .....   | vii  |
| <b>LIST OF TABLES</b> .....   | x    |
| <b>LIST OF FIGURES</b> .....  | xi   |
| <br>  |      |
| <b>CHAPTER I: INTRODUCTION</b>  |      |
| <b>1.1 Introduction</b> .....   | 1    |
| <b>1.2 Objectives and Scope</b> .....   | 2    |
| 1.2.1 Objectives .....  | 2    |
| 1.2.2 Scopes of research.....   | 2    |
| <br>  |      |
| <b>CHAPTER II: THEORY AND LITERATURE SURVEY</b>   |      |
| <b>2.1 Theory of Electrochemistry</b> .....   | 3    |
| 2.1.1 Cyclic Voltammetry.....   | 3    |
| 2.1.2 Amperometry.....  | 4    |
| 2.1.3 Flow injection analysis with electrochemical detection.....   | 4    |
| <b>2.2 Literature Survey</b> .....  | 6    |
| <b>2.2.1 Electroanalytical methods for determination of</b><br><b>sulfur-containing compounds</b> .....                     | 6    |
| 2.2.1.1 Differential pulse electrochemical detection.....   | 6    |
| 2.2.1.2 Amperometric detection with platinum microelectrode<br>chemically modified by copper tetraaminophthalocyanine ..... | 7    |
| 2.2.1.3 Mercury electrode.....  | 10   |



|   | Page      |
|---|-----------|
| 2.2.1.4 Bi(V)-Doped PbO <sub>2</sub> film electrode.....                                | 8         |
| <b>2.2.3 Boron-doped diamond thin film and its application in electrochemistry.....</b> | <b>15</b> |
| 2.2.3.1 Boron-doped diamond thin film and its properties.....                           | 15        |
| 2.2.3.2 Application of Boron-doped diamond thin films .....                             | 17        |
| <b>2.2.4 Flow injection analysis with diamond electrode.....</b>                        | <b>18</b> |
| 2.2.4.1 Fe(CN) <sub>6</sub> <sup>4-</sup> .....   | 18        |
| 2.2.4.2 Azide anion.....  | 20        |
| <br><b>CHAPTER III: EXPERIMENT</b>  |           |
| <b>3.1 Instruments and Equipment.....</b>   | <b>22</b> |
| <b>3.2 Apparatus for FI System.....</b>   | <b>22</b> |
| <b>3.3 Reagents.....</b>  | <b>24</b> |
| <b>3.4 The Preparation of Solutions.....</b>  | <b>25</b> |
| <b>3.5 Procedure .....</b>  | <b>28</b> |
| 3.5.1 The Oxidation of Sulfur-Containing Compounds.....                                 | 28        |
| 3.5.1.1 pH dependence.....  | 29        |
| 3.5.1.2 The anodic potential of sulfur-containing compounds.....                        | 29        |
| 3.5.1.3 The scan rate dependence study.....   | 29        |
| 3.5.1.4 The concentration dependence study.....   | 29        |
| 3.5.2 The Home-made Flow Cell.....  | 30        |
| 3.5.3 The Optimization of the FI System.....  | 31        |
| 3.5.4 Repeatability.....  | 32        |
| 3.5.5 Detection Limit.....  | 32        |
| 3.5.6 Comparison with Other Flow Cell.....  | 32        |
| <br><b>CHAPTER IV: RESULTS AND DISCUSSION</b>   |           |
| <b>4.1 The Oxidation of Sulfur Containing Compounds.....</b>                            | <b>33</b> |
| 4.1.1 pH Dependence.....  | 33        |
| 4.1.2 The Anodic Potential of Sulfur-Containing Compounds.....                          | 34        |



|  | Page      |
|--|-----------|
| 4.1.3 The Scan Rate Dependence Study.....                        | 44        |
| 4.1.4 The Concentration Dependence Study.....                    | 47        |
| <b>4.2 The Home-made Flow Cell.....</b>                          | <b>51</b> |
| <b>4.3 The optimization of the FI system.....</b>                | <b>52</b> |
| 4.3.1 The hydrodynamic measurement.....                          | 52        |
| <b>4.4 Repeatability.....</b>                                    | <b>57</b> |
| <b>4.5 Detection limit.....</b>                                  | <b>59</b> |
| <b>4.6 Comparison with the Other Flow Cell.....</b>              | <b>65</b> |
| <br>   |           |
| <b>CHAPTER V: CONCLUSION AND SUGGESTION FOR<br/>FURTHER WORK</b> |           |
| <b>5.1 Conclusion.....</b>                                       | <b>69</b> |
| 5.1.1 The oxidation of sulfur-containing compounds.....          | 69        |
| 5.1.2 Flow injection analysis.....                               | 69        |
| 5.1.3 A home-made flow cell.....                                 | 70        |
| <b>5.2. Suggestion for Further works.....</b>                    | <b>70</b> |
| <br>   |           |
| <b>REFERENCES.....</b>   | <b>71</b> |
| <b>CURRECULUM VITA.....</b>                                      | <b>73</b> |

สถาบันวิทยบริการ  
จุฬาลงกรณ์มหาวิทยาลัย

## LIST OF TABLES

| Table | Page  |
|-------|---|
| 2.1   | Analytical data of the five analytes.....10   |
| 2.2   | Summary of the diamond FIA-EC detector perform parameters<br>for ferrocyanide and ferricyanide.....20   |
| 3.1   | Listed of chemicals and suppliers.....24  |
| 4.1   | The oxidation potentials of cysteine in various pH.....34   |
| 4.2   | The peak potential and anodic peak current of oxidation of<br>1.0 mM sulfur-containing compounds from cyclic voltammetry<br>at scan rate 0.05 V/s, electrode area is 0.07 cm <sup>2</sup> .....40 |
| 4.3   | Sensitivity, linear range and limit of detection of<br>sulfur-containing compounds for boron-doped diamond thin-film<br>and glassy carbon electrodes.....50                                       |
| 4.4   | Peak variability of sulfur-containing compounds.....59  |
| 4.5   | The linear range, sensitivity, detection limit and peak variability<br>of sulfur-containing compounds.....64  |
| 4.6   | The linear range, sensitivity, detection limit and peak variability of<br>sulfur-containing compounds.....68  |

## LIST OF FIGURES

| Figure |   | Page |
|--------|---|------|
| 2.1    | (a) Cyclic potential sweep. (b) Resulting cyclic voltammogram   | 3    |
| 2.2    | Electrochemical detectors (S, sensitive surface): (a) annular sensor;<br>(b) cascade-type sensor; (c) wire-type sensor.....   | 5    |
| 2.3    | Microbore LC separation of glutathione and glutathione fragments.<br>LC condition: C18 1 mm UniCell column; 76 $\mu$ L/min; and mobile<br>phase 99.6% 0.1 M phosphate buffer (pH 3)/ 0.4% MeCN.....   | 7    |
| 2.4    | Cyclic voltammograms of the CuTAPc/Pt CME (a) in the blank<br>electrolyte, and (b) (a) + 1.0 mmol/l Cys. Electrolyte: 0.20 mol/l<br>phosphate buffer (pH 3.0). Scan rate: 100 mV/s.....   | 8    |
| 2.5    | (A) Three-dimensional hydrodynamic voltammogram and (B)<br>hydrodynamic voltammogram of mixture of (a) 2 nmol cysteine<br>(Cys), (b) 2 nmol ascorbic acid (AA), (c) 4 nmol glutathione (GSH),<br>(d) 2 nmol uric acid (UA) and (e) 2 nmol acetyl-cysteine (Acy) at the<br>CuTAPc/Pt CMEs in HPLC. Column: Zorbax C8 (4.0mm x 25 cm);<br>injection volume: 20 $\mu$ l; mobile phase: 0.20 mol/l phosphate buffer,<br>pH 3.0 ; flow rate: 1 ml/min..... | 9    |
| 2.6    | Cathodic stripping D.C. voltammetry of Hcys and Cys. Solutions of<br>10 $\mu$ M Hcys/Cys in 50 mM $\text{Na}_2\text{B}_4\text{O}_7$ , accumulation at +0.05 V for<br>180 s, scanning from +0.05 to -1.0 V at the rate of 20 $\text{mVs}^{-1}$ .<br>Hcys — , Cys ..... ..  | 11   |

| Figure  | Page |
|---|------|
| 2.7   | 13   |
| <p>Voltammetric response (positive scan) for (A) Cys, (B) GSH, (C) Cys<sub>2</sub>, (D) Met, and (E) MetSO at 1 : 2 Bi-PbO<sub>2</sub> rotated electrode in 0.1 M HClO<sub>4</sub>. Concentration (mM): (----) 0, (—) 1.0; scan rate: 40 mVs<sup>-1</sup>; rotational velocity: 262 rad s<sup>-1</sup>.....</p>   |      |
| 2.8   | 14   |
| <p>HPLC-EC results for sample containing 1.0 μM of Cys and 5.0 μM GSH, Met, MetSO, Hcys GSSG and Cys<sub>2</sub>. Mobile phase: 0.10 M HClO<sub>4</sub>/ 0.15 M NaClO<sub>4</sub>/ 5% MeCN at 1.0 mL min<sup>-1</sup>; column: Dionex OmniPac PCX-500 guard (4 x 250 mm); working electrode: 1:2 Bi-PbO<sub>2</sub>; detection potential: 1.60 V (vs. SSCE).....</p>      |      |
| 2.9   | 16   |
| <p>Cyclic voltammetric current versus potential curves for (A) boron-doped diamond thin film (inset shows capacitance versus potential profile for diamond thin-film electrode in 1 M KCl) and (B) glassy carbon and boron-doped diamond thin-film electrodes in 0.1 M KCl...</p>   |      |
| 2.10  | 17   |
| <p>Linear-sweep voltammetric current versus potential curve for a boron-doped diamond thin film electrode exposed to 1 mM N<sub>3</sub><sup>-</sup> in 0.1 M phosphate buffer at pH 7.2 showing total and background current.....</p>   |      |
| 2.11  | 19   |
| <p>(A) Hydrodynamic background I-E curve for a diamond film in 0.1M KCl at a flow rate 0.5 mL/min. The data were obtained at the end of a 30 min period at each potential. (B) Hydrodynamic i-E curve for the diamond film using 20 μL injections of 1 mM Fe(CN)<sub>6</sub><sup>4-</sup> in 0.1 M KCl. The mobile phase was 0.1 M KCl at a flow rate 0.5 mL/min.....</p> |      |

| Figure  | Page |
|---|------|
| 2.12 (A) Diamond thin-film response to 20 $\mu\text{L}$ injection of 0.1 mM $\text{N}_3^-$ in 0.1 M phosphate buffer, pH 7.2. Flow rate 1.0 mL/min. Detection potential 1.25 V. (B) A diamond thin-film response to 20 $\mu\text{L}$ injection of 0.3 $\mu\text{M}$ $\text{N}_3^-$ in 0.1 M phosphate buffer, pH 7.2. Same flow rate and detection potential as in A..... | 21   |
| 3.1 The compartments of cell: A) three neck glass cell, B) brass holder, C) boron-doped diamond thin-film electrode and D) neoprene o-ring..  | 23   |
| 3.2 The electrochemical cell for cyclic voltammetric study.....   | 28   |
| 3.3 The modified flow cell: (A) a side elevation of cell and (B) a top piece.....   | 30   |
| 3.4 The schematic diagram of FI system.....   | 31   |
| 4.1 Cyclic voltammogram of 0.1 M carbonate buffer pH 9.2, using boron-doped diamond thin-film electrode at scan rate 0.05 V/s from 0 to 1.3 V vs. Ag/AgCl. The area of electrode is 0.07 $\text{cm}^2$ .....  | 35   |
| 4.2 Cyclic voltammogram of 0.1 M carbonate buffer pH 9.2, using glassy carbon electrode at scan rate 0.05 V/s from 0 to 1.3 V vs. Ag/AgCl. The area of electrode is 0.07 $\text{cm}^2$ .....  | 35   |
| 4.3 Cyclic voltammogram of 1.0 mM cysteine in 0.1 M carbonate buffer pH 9.2 using boron-doped diamond thin-film electrode at scan rate 0.05 V/s from 0 to 1.1 V vs. Ag/AgCl. The area of electrode is 0.07 $\text{cm}^2$ . (—) first scan, (---) second scan and (···) background.....  | 37   |

| Figure   | Page |
|--|------|
| 4.4  | 37   |
| <p>Cyclic voltammogram of 1.0 mM cysteine in 0.1 M carbonate buffer pH 9.2 using glassy carbon electrode at scan rate 0.05 V/s from 0 to 1.1 V vs. Ag/AgCl. The area of electrode is 0.07 cm<sup>2</sup>. (—) first-scan, (---) second scan and (····) background.....</p>   |      |
| 4.5  | 38   |
| <p>Cyclic voltammogram of 1.0 mM ampicillin in 0.1 M carbonate buffer pH 9.2 using glassy carbon electrode at scan rate 0.05 V/s from 0 to 1.1 V vs. Ag/AgCl. The area of electrode is 0.07 cm<sup>2</sup>. (—) first scan, (---) second scan and (····) background.....</p>   |      |
| 4.6  | 39   |
| <p>Cyclic voltammogram of (A) 1.0 mM cystamine in 0.1 M carbonate buffer pH 9.2, (B) carbonate buffer pH 9.2 using boron-doped diamond thin-film electrode at scan rate 0.05 V/s from 0.5 to 1.3 V vs. Ag/AgCl. The area of electrode is 0.07 cm<sup>2</sup> and (C) subtracted voltammogram of (A) and (B).....</p>   |      |
| 4.7  | 43   |
| <p>Structures of sulfure-containing compounds: (A) cysteine, (B) homocysteine, (C) glutathione, (D) 2-mercaptoethane sulfonic acid and (E) cephalixin.....</p>   |      |
| 4.8  | 45   |
| <p>Cyclic voltammogram of 10.0 mM cephalixin in 0.1 M carbonate buffer pH 9.2 using boron-doped diamond thin-film electrode, potential range from 0 to 1.1 V vs. Ag/AgCl. The area of electrode is 0.07 cm<sup>2</sup>: (—■—) scan rate 0.20 V/s, (—◇—) scan rate 0.10 V/s, (—▲—) scan rate 0.05 V/s, (—●—) scan rate 0.02 V/s and (—▽—) background current at scan rate 0.05 V/s.....</p> |      |

| Figure   | Page |
|--|------|
| 4.9 (scan rate) <sup>1/2</sup> vs current of 10.0 mM cephalixin in 0.1 M carbonate buffer pH 9.2 using boron-doped diamond thin-film electrode. The area of electrode is 0.07 cm <sup>2</sup> .....  | 46   |
| 4.10 Cyclic voltammograms for boron-doped diamond thin-film electrode in pH 9.2 carbonate buffer for a series of homocysteine concentration: 0, 0.48, 1.01, 1.03, 50.7 and 10.1 mM. Potential sweep rate, 100 mV/s; electrode area, 0.07 cm <sup>2</sup> .....                                       | 48   |
| 4.11 Cyclic voltammograms for glassy carbon electrode in pH 9.2 carbonate buffer for a series of homocysteine concentration: 0, 0.48, 1.01, 1.03, 50.7 and 10.1 mM. Potential sweep rate, 100 mV/s; electrode area, 0.07 cm <sup>2</sup> .....   | 48   |
| 4.12 The calibration curves of homocysteine in 0.1 M carbonate buffer 9.2 pH using (○) boron-doped diamond thin-film and (□) glassy carbon electrodes. Potential sweep rate, 100 mV/s; electrode area, 0.07 cm <sup>2</sup> . The correlation coefficients were 0.9988 and 0.9922, respectively..... | 49   |
| 4.13 The modified flow cell.....   | 51   |
| 4.14 The completed home-made flow cell.....  | 51   |
| 4.15 Background hydrodynamic <i>i</i> - <i>E</i> curve for boron-doped diamond thin-film electrode in 0.1 M carbonate buffer, pH 9.2. Flow rate 1.0 mL/min. Each datum was recorded at the end of a 2 min period...  | 53   |



| Figure | Page   |    |
|--------|--|----|
| 4.16   | Hydrodynamic <i>i-E</i> curve for boron-doped diamond thin-film electrode exposed to 20- $\mu$ L injection of 50 $\mu$ M cysteine in 0.1 M carbonate buffer, pH 9.2. Flow rate 1.0 mL/min. Each datum represents the average of 10 injections.....                                   | 54 |
| 4.17   | Hydrodynamic <i>i-E</i> curve for boron-doped diamond thin-film electrode exposed to 20- $\mu$ L injection of 50 $\mu$ M homocysteine in 0.1 M carbonate buffer, pH 9.2. Flow rate 1.0 mL/min. Each datum represents the average of 10 injections.....                               | 55 |
| 4.18   | Hydrodynamic after correcting background for boron-doped diamond thin-film electrode exposed to 20- $\mu$ L injection of 50 $\mu$ M homocysteine in 0.1 M carbonate buffer, pH 9.2. Flow rate 1.0 mL/min. Each datum represents the average of 10 injections.....                    | 55 |
| 4.19   | Hydrodynamic after correcting background for boron-doped diamond thin-film electrode exposed to 20- $\mu$ L injection of 50 $\mu$ M 2-mercaptoethane sulfonic acid in 0.1 M carbonate buffer, pH 9.2. Flow rate 1.0 mL/min. Each datum represents the average of 10 injections.....  | 56 |
| 4.20   | Diamond thin-film response to 10 20- $\mu$ L injections of (A) 10 $\mu$ M cysteine, (B) 50 $\mu$ M homocysteine and (C) 50 $\mu$ M 2-mercaptoethane sulfonic acid in 0.1 M carbonate buffer, pH 9.2. Flow rate 1.0 mL/min. Detection potential 0.55, 0.775 and 0.625, respectively.. | 58 |

| Figure | Page   |    |
|--------|--|----|
| 4.21   | Diamond thin-film response to 5 20- $\mu$ L injections of 100 nM cysteine, in 0.1 M carbonate buffer, pH 9.2. Flow rate 1.0 mL/min. Detection potential 0.55 V.....  | 60 |
| 4.22   | Calibration curve of cysteine in 0.1 M carbonate buffer, pH 9.2 by flow injection analysis. Flow rate 1.0 mL/min. Detection potential 0.55 V.....  | 61 |
| 4.23   | Diamond thin-film response to 10 20- $\mu$ L injections of 200 nM homocysteine, in 0.1 M carbonate buffer, pH 9.2. Flow rate 1.0 mL/min. Detection potential 0.775 V.....  | 62 |
| 4.24   | Calibration curve of homocysteine in 0.1 M carbonate buffer, pH 9.2 by flow injection analysis. Flow rate 1.0 mL/min. Detection potential 0.775 V.....   | 62 |
| 4.25   | Diamond thin-film response to 5 20- $\mu$ L injections of 100 nM 2-mercaptoethane sulfonic acid, in 0.1 M carbonate buffer, pH 9.2. Flow rate 1.0 mL/min. Detection potential 0.625 V.....                                   | 63 |
| 4.26   | Calibration curve of 2-mercaptoethane sulfonic acid in 0.1 M carbonate buffer, pH 9.2 by flow injection analysis. Flow rate 1.0 mL/min. Detection potential 0.625 V.....   | 64 |
| 4.27   | Signals of background hydrodynamic study of 0.1 M carbonate buffer, pH 9.2 using boron-doped diamond thin-film with home-made flow cell. Flow rate 1.0 mL/min. The sharply pulled signal occurred from potential change..... | 65 |

| Figure | Page   |    |
|--------|--|----|
| 4.28   | Background and 50 $\mu\text{M}$ 2-mercaptoethane sulfonic acid hydrodynamic <i>i-E</i> curves for boron-doped diamond thin-film electrode with home-made flow cell in 0.1 M carbonate buffer, pH 9.2. Flow rate 1.0 mL/min.....  | 66 |
| 4.29   | Diamond thin-film response to 5 20- $\mu\text{L}$ injections of 10 $\mu\text{M}$ 2-mercaptoethane sulfonic acid for boron-doped diamond thin-film electrode with home-made flow cell in 0.1 M carbonate buffer, pH 9.2. Flow rate 1.0 mL/min. Detection potential 0.625 V..... | 67 |
| 4.30   | Calibration curve of 2-mercaptoethane sulfonic acid in 0.1 M carbonate buffer, pH 9.2 by flow injection analysis with home-made flow cell.....   | 68 |

# CHAPTER I

## INTRODUCTION

### 1.1 Introduction

Many sulfur-containing compounds are of great biological and clinical significance. Examples include the amino acids cysteine (Cys), cystine (Cys<sub>2</sub>), methionine (Met) and homocysteine (Hcys), as well as simple peptides containing Cys and Met, e.g., glutathione in its reduced form (GSH). Other examples of sulfur-compounds are 2-mercaptoethane sulfonic acid, coenzymeM, cephalixin, and antibiotic drug. In particular, these compounds and the products of their metabolism have recently been studied intensively because of medical reports of the link between level of homocysteine in blood and cardiovascular diseases [1]. Quantitative determination of these compounds is commonly performed by high performance liquid chromatography (HPLC) with fluorescence or UV/Visible absorbance detection after derivatization with a suitable chromophoric or fluorophoric functional groups [2].

In order to avoid tedious derivatization steps in the determination of sulfur-containing amino acids and peptides, Vanderburg and Johnson developed a direct detection method based on pulsed electrochemical detection (PED) [3]. The detection of sulfur-containing compounds with electrochemical detection is of higher sensitive than fluorometry and has a lower cost. Recently, many electrochemical methods for determination of sulfur-containing compounds have been reported and the differences between these reports involve the types of measurement and types of electrode.

## 1.2 Objectives and Scope

### 1.2.1 Objectives

1.2.1.1 To compare the electrochemical properties of sulfur-containing compounds between two working electrodes which are a boron-doped diamond thin-film and a glassy carbon electrodes.

1.2.1.2 To modify a flow system for quantitative study of sulfur-containing compounds using a boron-doped diamond thin-film electrode as a detector.

1.2.1.3 To find the optimal condition for the analysis of sulfur-containing compounds at low concentration.

### 1.2.2 Scope of the research

1.2.2.1 To study the electrochemical properties of sulfur-containing compounds consisting of cysteine, homocysteine, glutathione and 2-mercaptoethane sulfonic acid, etc., using boron-doped diamond thin-film electrodes with cyclic voltammetry and to compare the results, with those from glassy carbon electrode.

1.2.2.2 To modify a flow system, including the flow cell and flow channel for a boron-doped diamond thin-film for the analysis of sulfur-containing compounds. This flow cell should be easy to clean, easy to change electrodes and give a reproducible signal.

1.2.2.3 To find the optimal condition, using a boron-doped diamond thin-film electrode as a detector for flow injection analysis. The following parameters such as potential amperometric detection, flow rate, decrease of adsorption on surface of electrode, etc. were studied.

## CHAPTER II

### THEORY AND LITERATURE SURVEY

#### 2.1 Theory of Electrochemistry

##### 2.1.1 Cyclic Voltammetry

Cyclic voltammetry is an important electrochemical method. It like linear sweep voltammetry that there are increment potential (in positive or negative way) in linear relation and measure current. In addition, cyclic votammetry has reversed potential scan to starting potential (Figure 2.1a). So the cyclic voltammogram, for reversible reaction, will has an oxidation and a reduction peaks as shown in Figure 2.1b. Cyclic voltammetry is a very popular technique for initial electrochemical studies of new systems and has proven very useful in obtaining more information about fairly complicated electrode reactions.

สถาบันวิทยบริการ  
จุฬาลงกรณ์มหาวิทยาลัย

Figure 2.1 (a) Cyclic potential sweep. (b) Resulting cyclic voltammogram

### 2.1.2 Amperometry

Amperometry is an electrochemical technique for quantitation. A potential is held and a current was measured. When a concentration of an electroactive species change, like in titration and flow injection, the current will change.

### 2.1.3 Flow Injection Analysis with Electrochemical Detection

Flow injection analysis with electrochemical detection, on the other hand, relies on transport of an electroactive species toward an electrochemically active surface. If the species is effectively transferred from the bulk solution to the diffusion layer and across the diffusion layer to the sensing surface, it can be sensed. This is why, in FIA, where the sample zone is stratified, the species to be measured may in extreme cases pass the ion-sensitive surface unmonitored. This is most likely to happen when the measuring channel is straight (Figure 2.9 a) [9], and is nearly certain if the sensitive surface (S) is, because of faulty construction, recessed in the wall. The wall-jet construction, well-known in polarography and voltammetry, changes the direction of flow so that the stream impinges on the sensitive surface attached perpendicularly to the end of the tube. A cascade type of flow cell (Figure 2.9 b) is a further extension of this principle. A wire-type detector is the most effective to probe the center of the zone (Figure 2.9 c) but also the most awkward to construct.



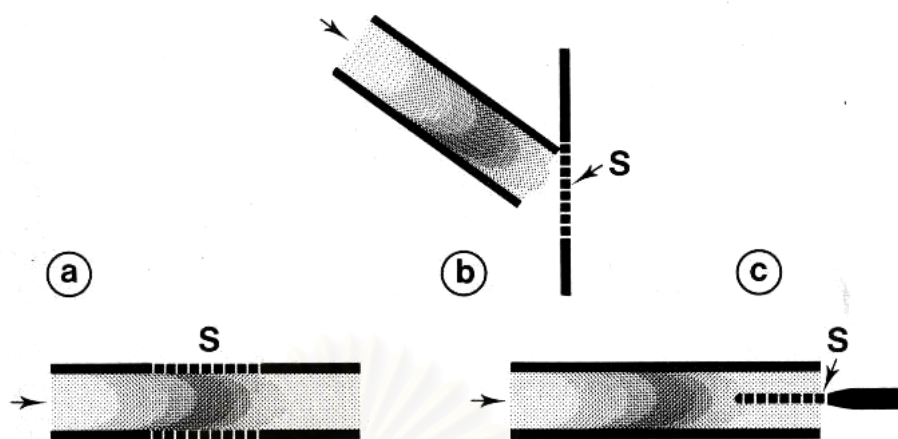


Figure 2.3 Electrochemical detectors (S, sensitive surface): (a) annular sensor; (b) cascade-type sensor; (c) wire-type sensor.

## 2.2 Literature Survey

### 2.2.1 Electroanalytical Methods for The Determination of Sulfur-Containing Compounds

#### 2.2.1.1 Differential pulse electrochemical detection

Pulse electrochemical detection (PED) is a useful technique for the detection of sulfur-containing compound[4]. Sulfur-containing compounds were separated by microbore liquid chromatography and were detected by PED (Figure 2.). Both thiols and disulfides can be detected directly at a single gold electrode with limits of detection at the low picomolar level. In this study, two common PED techniques, pulsed amperometric detection (PAD) and integrated pulsed amperometric detection (IPAD), were investigated using model sulfur-containing compounds. Although both techniques could be used, it was found that IPAD resulted in better sensitivity and baseline stability than PAD.

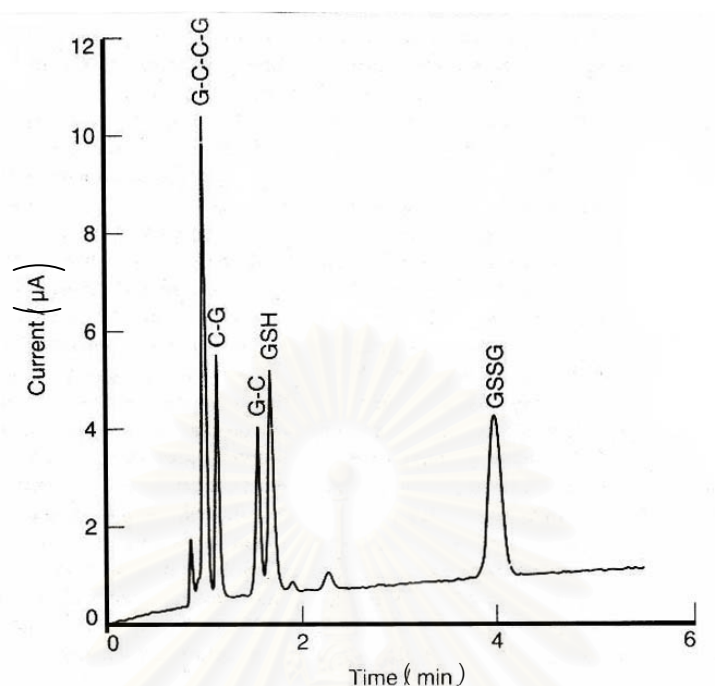


Figure 2.3 Microbore LC separation of glutathione and glutathione fragments.

LC condition: C18 1 mm UniCell column; 76  $\mu\text{L}/\text{min}$ ; and mobile phase 99.6% 0.1 M phosphate buffer (pH 3)/ 0.4% MeCN [4].

#### 2.2.1.2 Amperometric detection with platinum microelectrode chemically modified by copper tetraaminophthalocyanine

Amperometric methods are widely used for the detection of electrochemically oxidizable and reducible substances in liquid chromatography. However amperometric detection of sulfur-containing compounds is often hampered by slow electron-transfer kinetics at the electrode surface[5]. As a result, oxidation occurs at a potential that is larger than the expected thermodynamic potential. Both the selectivity and limits of detection of the electrochemical measurements are greatly dependent on the magnitude of the applied overpotentials. Chemically modified

electrodes (CMEs) can overcome this problem through the use of surface-bound redox mediator. Copper tetraaminophthalocynine on 200  $\mu\text{M}$  platinum (CuTAPc/Pt) CME has been used as detector for determining thiocompounds in human whole blood with HPLC (Figure 2.4).

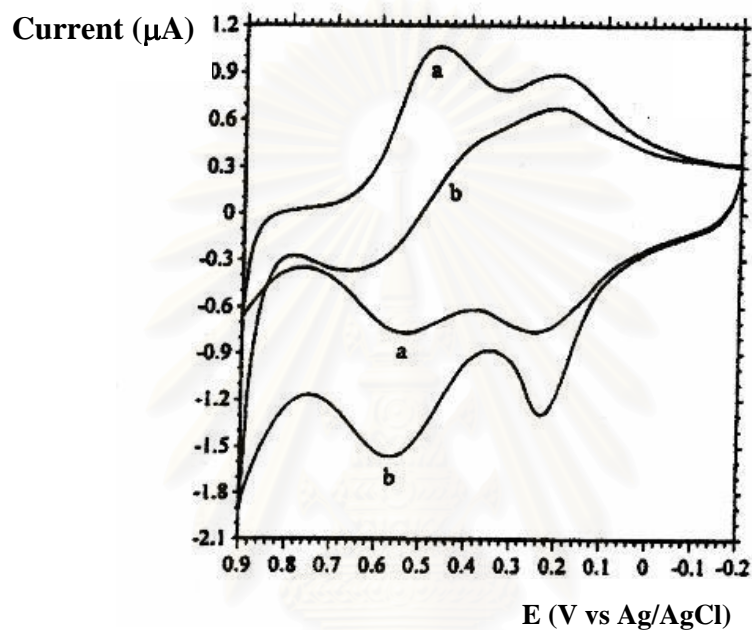


Figure 2.4 Cyclic voltammograms of the CuTAPc/Pt CME (a) in the blank electrolyte, and (b) (a) + 1.0 mmol/l Cys. Electrolyte: 0.20 mol/l phosphate buffer (pH 3.0). Scan rate: 100 mV/s [5].

สถาบันวิทยบริการ  
จุฬาลงกรณ์มหาวิทยาลัย

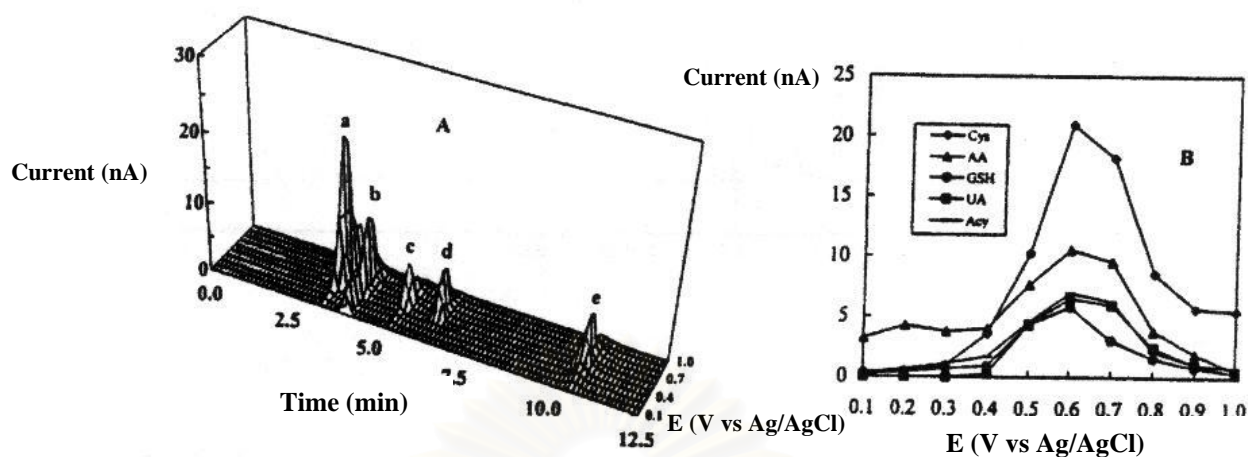


Figure 2.5 (A) Three-dimensional hydrodynamic voltammogram and

(B) hydrodynamic voltammogram of mixture of

- (a) 2 nmol cysteine (Cys),
- (b) 2 nmol ascorbic acid (AA),
- (c) 4 nmol glutathione (GSH),
- (d) 2 nmol uric acid (UA) and
- (e) 2 nmol acetyl-cysteine (Acy)

at the CuTAPc/Pt CMEs in HPLC. Column: Zorbax C8 (4.0mm x 25 cm); injection volume: 20  $\mu$ l; mobile phase: 0.20 mol/l phosphate buffer, pH 3.0 ; flow rate: 1 ml/min [5].

The linearity of the five compounds at CuTAPc/Pt CME in HPLC, is in a set of standard solutions, is found to be over three orders of magnitude.

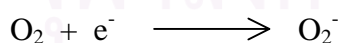
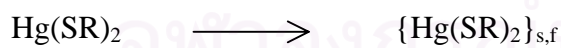
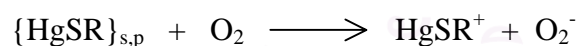
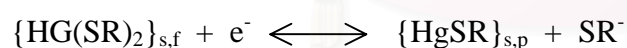
Correlation coefficients are larger than 0.99. The analytical data are summarized in Table 2.1.

Table2.1 Analytical data of the five analytes

| Compounds | Regression equation | R <sup>2</sup> | Linear range (mol/l)                      | LOD (pmol) |
|-----------|---------------------|----------------|---|------------|
| Cys       | $Y=0.09+20.81x$     | 0.9995         | $8.0 \times 10^{-7} - 1.0 \times 10^{-3}$ | 10         |
| GSH       | $Y=0.05+2.84x$      | 0.9991         | $1.0 \times 10^{-6} - 1.0 \times 10^{-3}$ | 16         |
| Acy       | $Y=0.06+6.93x$      | 0.9989         | $1.0 \times 10^{-6} - 1.0 \times 10^{-3}$ | 16         |
| AA        | $Y=0.11+10.43x$     | 0.9994         | $8.0 \times 10^{-7} - 1.0 \times 10^{-3}$ | 10         |
| UA        | $Y=0.08+6.43x$      | 0.9988         | $1.0 \times 10^{-6} - 1.0 \times 10^{-3}$ | 16         |

### 2.2.1.3 Mercury electrode

The electrochemical reactivity of homocysteine at mercury electrodes was studied with cysteine[6]. The report showed that homocysteine differs from cysteine in electrochemical behavior due to slight differences in hydrophobicity. This was apparent in adsorptivity, in anodic reactions with mercury, are in catalytic reduction of oxygen mediated by mercury thiolates.



(the subscript 's' denotes here the adsorbed state with the bound thiol in flat, 'f', or perpendicular, 'p', orientation)

When the mercurous thiolate is being reduced to metallic mercury, the catalytic effect disappears. The results for homocysteine and cysteine are shown in Figure 2.6

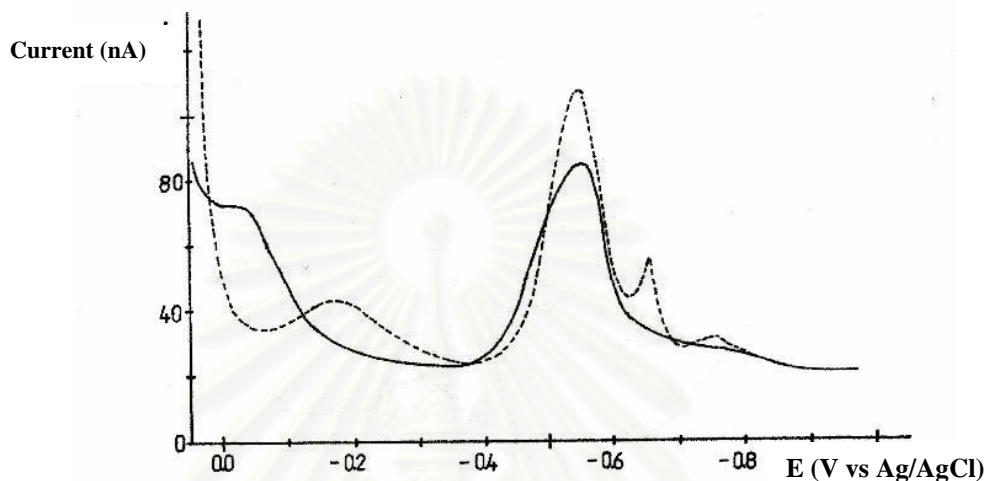


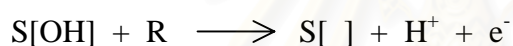
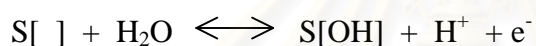
Figure 2.6 Cathodic stripping D.C. voltammetry of Hcys and Cys Solutions of 10  $\mu\text{M}$  Hcys/Cys in 50 mM  $\text{Na}_2\text{B}_4\text{O}_7$ , accumulation at +0.05 V for 180 s, scanning from +0.05 to  $-1.0$  V at the rate of  $20 \text{ mVs}^{-1}$ . Hcys: —, Cys: ..... [6].

#### 2.2.1.4 Bi(V)-Doped $\text{PbO}_2$ film electrode

Electroanalytic oxidation of sulfur-containing amino acids and peptides at Bi(V)-doped  $\beta\text{-PbO}_2$  film electrodes ( $\text{Bi-PbO}_2$ ) was investigated in acidic media and tested for amperometric detection of representatives of these compounds [7]. The  $\text{Bi-PbO}_2$  film electrodes permit detection with similar sensitivities for compounds that contain sulfhydryl, disulfide, thioether, and sulfoxide moieties. The results of oxidation of sulfur-containing compounds by linear sweep voltammetry are shown in Figure 2.7. There were also good results when applied to HPLC-EC (Figure 2.8).



For the redox mechanism of sulfur-containing compounds, it has been proposed that a prerequisite for anodic O-transfer reaction at Bi (V)-doped PbO<sub>2</sub>-film electrodes is the anodic discharge of H<sub>2</sub>O at PbO<sub>2</sub> sites to produce adsorbed OH radicals. S[OH] represents adsorbed OH radicals and S[ ] corresponds to unoccupied surface sites. Then, the O-transfer step is occurred. R is the reactant and RO is the product of O-transfer reaction. According to this mechanism, the adsorbed OH radical is the immediate source of the O-atom transferred to the oxidation product. The OH radical also is the precursor in the O<sub>2</sub>-evolution reaction, a fact that can diminish the current efficiency for desired O-transfer reaction, as represented by:



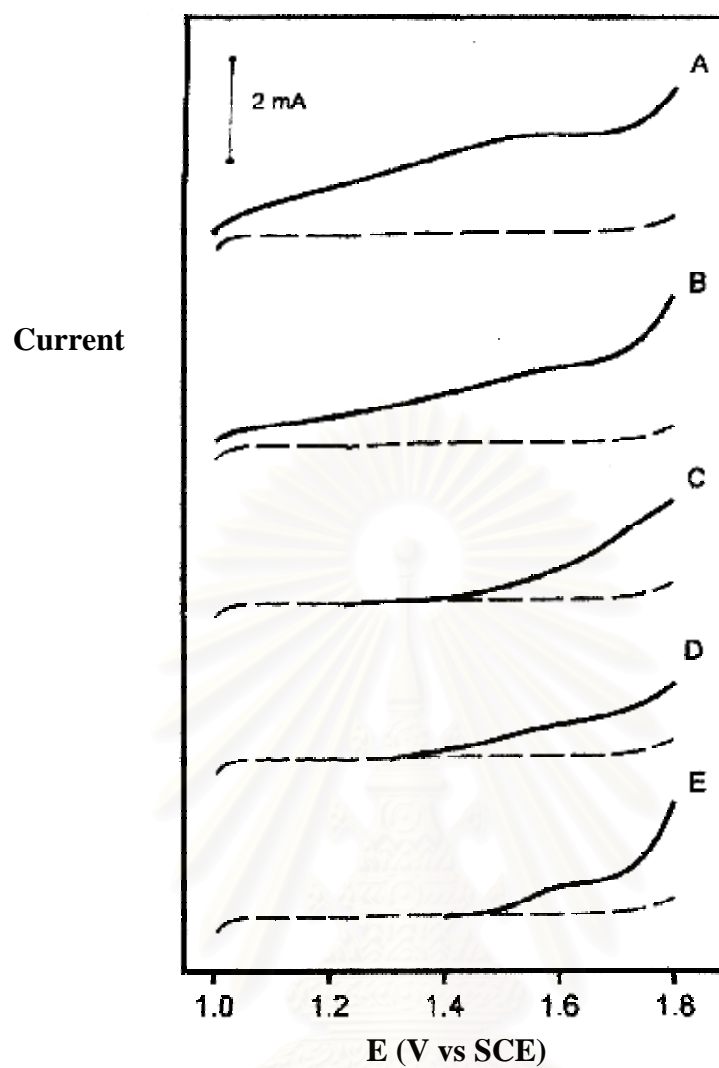


Figure 2.7 Voltammetric response (positive scan) for (A) Cys, (B) GSH, (C)  $\text{Cys}_2$ ,

(D) Met, and (E) MetSO at 1 : 2 Bi-PbO<sub>2</sub> rotated electrode in 0.1 M HClO<sub>4</sub>.

Concentration (mM): (----) 0, (—) 1.0; scan rate: 40 mVs<sup>-1</sup>;

rotational velocity: 262 rad s<sup>-1</sup> [7].

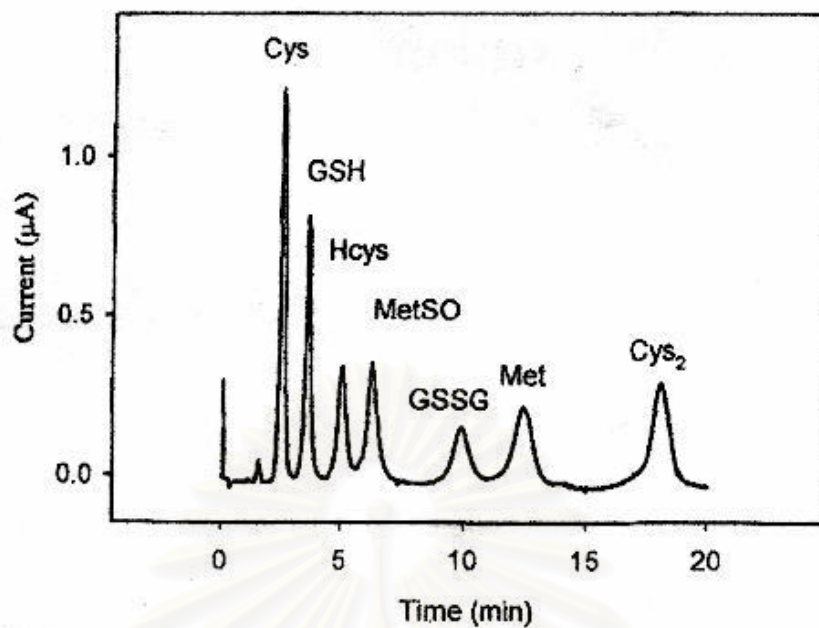


Figure 2.8 HPLC-EC results for sample containing 1.0  $\mu\text{M}$  of Cys and 5.0  $\mu\text{M}$  GSH, Met, MetSO, Hcys GSSG and Cys<sub>2</sub>. Mobile phase: 0.10 M HClO<sub>4</sub>/ 0.15 M NaClO<sub>4</sub>/ 5% MeCN at 1.0 mL min<sup>-1</sup>; column: Dionex OmniPac PCX-500 guard (4 x 250 mm); working electrode: 1:2 Bi-PbO<sub>2</sub>; detection potential: 1.60 V (vs. SCE) [7].

In the acidic media used in this study, only the non-sulfur containing amino acid tryptophane and tyrosine produced an anodic response; however, this occurred only at concentrations > 50  $\mu\text{M}$ .

สถาบันวิทยบริการ  
จุฬาลงกรณ์มหาวิทยาลัย

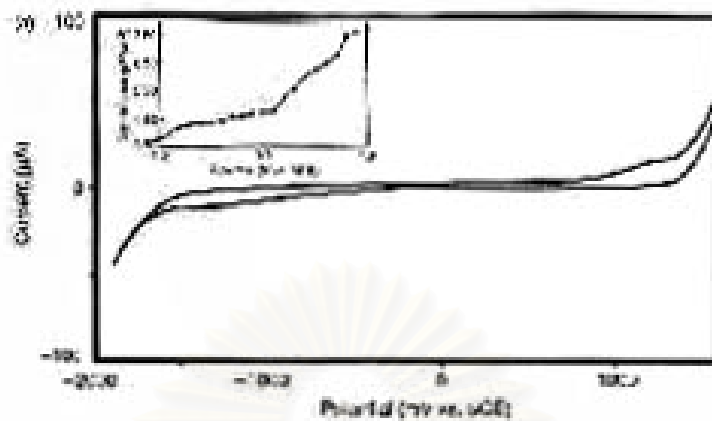
## 2.2.3 Boron-Doped Diamond Thin-Film and Its Application in Electrochemistry.

### 2.2.3.1 Boron-doped diamond thin film and its properties

Boron-doped diamond thin film is a synthetic conductive diamond. Each carbon atom in the film is tetrahedrally bonded to four other carbons using  $sp^3$ -hybrid orbitals. Microstructurally, the atoms arrange themselves in stacked, six-membered rings, with each ring in a chair rather than a planar conformation. The boron impurity atoms substitute in place of some of carbon atoms during film growth. Boron-doped diamond thin film possesses many of the superb physical properties of diamond such as extreme hardness, chemical inertness and high thermal conductivity.

Several electrochemically important properties distinguish boron-doped diamond thin films from conventional carbon electrodes. This material has many interesting electrochemical properties, which have been found to include the followings: (i) a low and stable voltammetric background current (about a factor of 10 less than that of polished glassy carbon for a similar geometric area as shown in Figure 2.9), (ii) a wide working potential window in aqueous electrolyte solutions, (iii) reversible to quasireversible electron transfer kinetics for the inorganic redox analytes  $Fe(CN)_6^{3-}/Fe(CN)_6^{4-}$ ,  $IrCl_6^{2-}/IrCl_6^{23-}$ , and  $Ru(NH_3)_6^{2+}/Ru(NH_3)_6^{3+}$  without any conventional surface pretreatment, (iv) enhanced S/B ratios for these analytes in voltammetric measurement because of the low background current, (v) slightly polar organic compound adsorption, and (vi) resistance to deactivation as some films have been observed to exhibit a relatively unchanging  $E_p$  for  $Fe(CN)_6^{3-}/Fe(CN)_6^{4-}$  over a 1 month period of exposure to the laboratory atmosphere. [8]

A)



B)

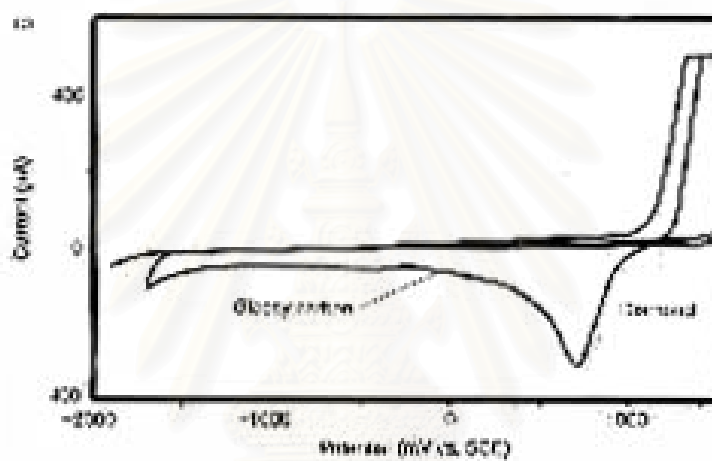


Figure 2.9 Cyclic voltammetric current versus potential curves for (A) boron-doped diamond thin film (inset shows capacitance versus potential profile for diamond thin-film electrode in 1 M KCl) and (B) glassy carbon and boron-doped diamond thin-film electrodes in 0.1 M KCl [8].

### 2.2.3.2 Application of boron-doped diamond thin-films

The detection of sodium azide using the boron-doped diamond thin-films has been studied [8]. Sodium azide, which is currently being phased out as a propellant for airbags, is not normally found in water supplies. However, as current-model cars containing azide-based airbags are retired, the likelihood of azide contamination of groundwater will increase significantly. GC, ion chromatography, and capillary electrophoresis detect azide anion with limits in the high-ppb to low-ppm range.

However, azide anion is electrochemically active at carbon (diamond and graphite), platinum, and gold electrodes. Figure 2.10 shows a linear-sweep voltammetric current versus potential curve for a boron-doped diamond thin film in 1.0 mM  $\text{NaN}_3$  + 0.1 M phosphate buffer, pH 7.2. Diamond gives a peak-shaped faradaic response for the oxidation of azide superimposed on a low, stable background current. Plots of the peak current versus the azide solution concentration were linear from 0.003 down to  $10^{-6}$  M, an analytical useful response for this analyte.

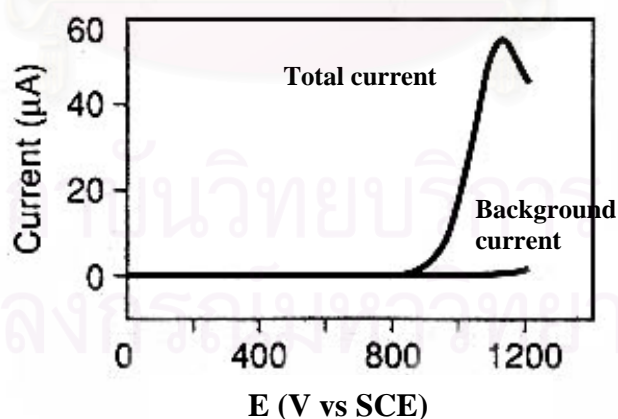


Figure 2.10 Linear-sweep voltammetric current versus potential curve for a boron-doped diamond thin film electrode exposed to 1 mM  $\text{N}_3^-$  in 0.1 M phosphate buffer at pH 7.2 showing total and background current [8].

The response for diamond remained unchanged even after weeks of exposure to laboratory air and was unaffected by  $F^-$ ,  $Cl^-$ ,  $NO_3^-$ , and AQDS in solution. By comparison, the faradaic signals for diamond and freshly polished glassy carbon were most often within 5% of each other, whereas the background currents were always a factor of 5 to 100 larger for glassy carbon. This means an enhanced S/B for diamond. In fact, S/B for diamond thin films is 38 to 50 larger than the ratio for glassy carbon at the 0.1 mM azide concentration level. The enhanced S/B leads to lower detection limits and results from the sizable lower residual background current for boron-doped diamond at the azide oxidation potentials.

## 2.2.4 Flow Injection Analysis with Diamond Electrode

### 2.2.4.1 $Fe(CN)_6^{4-}$

The redox reaction of  $Fe(CN)_6^{4-}$  has been studied by cyclic voltammetry, hydrodynamic voltammetry, and flow injection analysis with electrochemical detection (FIA-ED) at boron-doped diamond films without any prior surface pretreatment[10]. A thin-layer flow cell was used in this work. The results indicate that diamond films produce analytically useful responses in both scanning and constant potential modes (Table 2.2). Boron-doped diamond can be used as a substrate for the detection of both oxidation and reduction reactions.



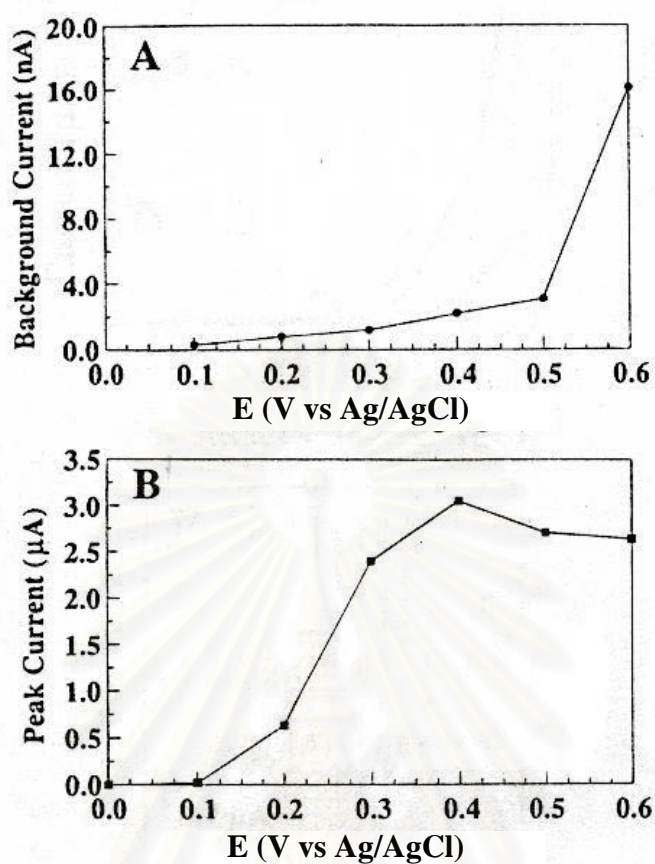


Figure 2.11 (A) Hydrodynamic background i-E curve for a diamond film in 0.1 M KCl at a flow rate 0.5 mL/min. The data were obtained at the end of a 30 min period at each potential. (B) Hydrodynamic i-E curve for the diamond film using 20  $\mu\text{L}$  injections of 1 mM  $\text{Fe}(\text{CN})_6^{4-}$  in 0.1 M KCl. The mobile phase was 0.1 M KCl at a flow rate 0.5 mL/min [10].

Table 2.2 Summary of the diamond FIA-EC detector perform parameters for hexacyanoferrate(II) and hexacyanoferrate(III) [9]

| <b>Hexacyanoferrate(II)</b>  |   |
|------------------------------|---|
| linear dynamic range         | $1 \times 10^{-3} - 1 \times 10^{-6} \text{ M}$ ( $r > 0.995$ ) |
| limit of detection (S/B = 3) | $2.05 \times 10^{-7} \pm 0.651 \text{ M}$ ( $n = 7$ )           |
| sensitivity                  | $7.04 \pm 0.656 \text{ nA}/\mu\text{M}$ ( $r > 0.995$ )         |
| peak height variability      | $13.3 \pm 4.05\%$ ( $n = 7$ )                                   |
| <b>Hexacyanoferrate(III)</b> |   |
| linear dynamic range         | $1 \times 10^{-3} - 1 \times 10^{-6} \text{ M}$ ( $r > 0.995$ ) |
| limit of detection (S/B = 3) | $5.73 \times 10^{-7} \pm 2.95 \text{ M}$ ( $n = 3$ )            |
| sensitivity                  | $11.9 \pm 7.63 \text{ nA}/\mu\text{M}$ ( $r > 0.998$ )          |
| peak height variability      | $11.1 \pm 7.63\%$ ( $n = 3$ )                                   |

#### 2.2.4.2 Azide anion

The oxidation of dissolved inorganic azide anion in aqueous media was investigated using high-quality, boron-doped diamond thin-film electrodes [11]. Linear sweep and differential pulse voltammetry, along with flow injection analysis in the amperometric detection mode, were used to study the reaction at neutral pH as a function of the potential sweep rate, analyte concentration, and electronic position. The flow injection analysis results for diamond showed reproducible peaks (Figure 2.12) and indicated a linear dynamic range of 3 orders of magnitude and a detection limit of 8 nM (0.3 ppb) at a S/N = 3. The diamond response was generally reproducible from film to film, and the background current signal and signal-to-background ratio were extremely stable for up to 12 h of continuous use. The results demonstrate that this electrode serves as an analytically useful substrate for detection of azide anion and exhibits superior performance characteristics compared with glassy carbon.

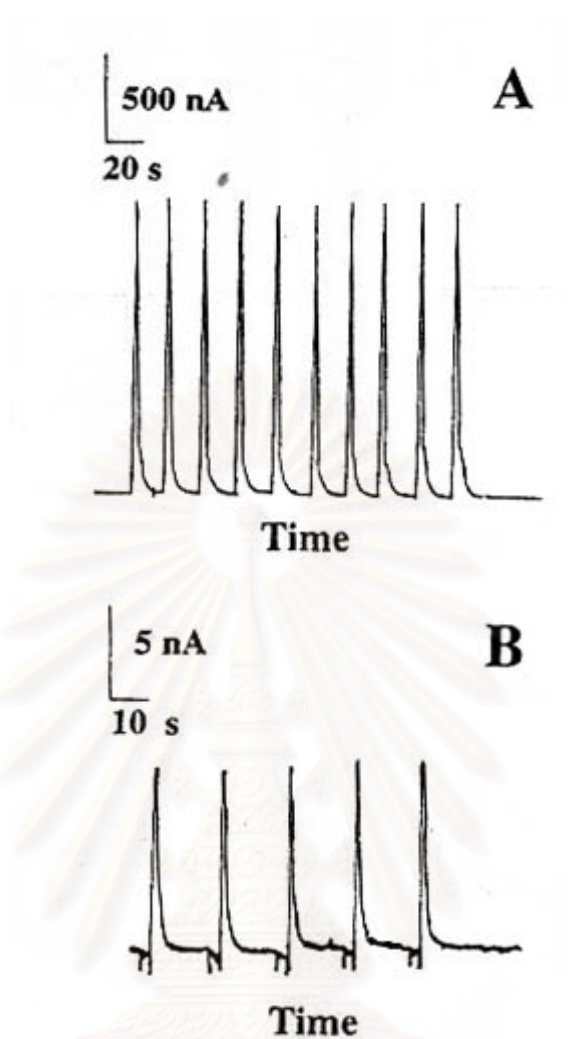


Figure 2.12 (A) Diamond thin-film response to 20  $\mu\text{L}$  injection of 0.1 mM  $\text{N}_3^-$  in 0.1 M phosphate buffer, pH 7.2. Flow rate 1.0 mL/min. Detection potential 1.25 V. (B) A diamond thin-film response to 20  $\mu\text{L}$  injection of 0.3  $\mu\text{M}$   $\text{N}_3^-$  in 0.1 M phosphate buffer, pH 7.2. Same flow rate and detection potential as in (A) [11].

## CHAPTER III

### EXPERIMENTAL

#### 3.1 Instruments and Equipment

The following are lists of general instruments and equipment employed for this study.

3.1.1 A Sonicator (USA) was used for cleaning the diamond electrode surface.

3.1.2 An analytical balance (Metler, Switzerland), was used for weighing chemicals in the preparation of all solutions of sulfur-containing compounds and of the carbonate buffer solution.

3.1.3 A pH meter (Metromh, Switzerland), was used for measuring pH value in the preparation of the carbonate buffer solution.

3.1.4 An Autolab Potentiostat, model Potentiostat 100 (Switzerland), was used for electrochemical measuring in cyclic voltammetric and amperometric measurements in flow injection analysis.

3.1.5 Boron-Doped Diamond thin films (BDD)

All boron-doped diamond thin-films were grown in the Fujishima laboratory at the University of Tokyo, and contained  $10^4$  ppm boron.

3.1.6 An Ag/AgCl electrode, TCI (Japan), was used as the reference electrode.

3.2.7 A BAS Glassy carbon (USA) was used as the working electrode.

3.2.8 A home-made platinum wire was used as the counter electrode.

3.2.9 A home-made glass cell and brass holder.

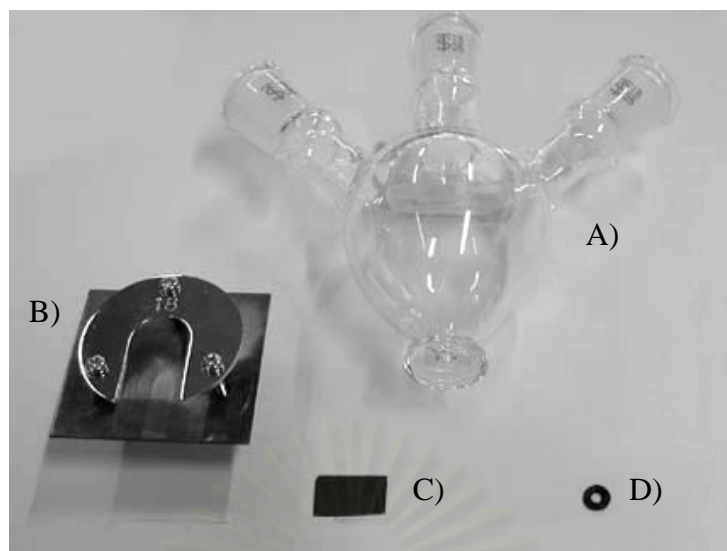


Figure 3.1 The compartments of cell: A) three neck glass cell, B) brass holder, C) boron-doped diamond thin-film electrode and D) neoprene o-ring

3.2.10 A BAS Polishing set, 0.5  $\mu\text{m}$  and 1.0  $\mu\text{m}$  diamond slurry, was used for polishing the surface of the glassy carbon electrode.

### 3.2 Apparatus for Flow Injection (FI) System

The FI system, in this work, includes the following equipments:

3.2.1 A reagent delivery module, Water (USA), was used for driving carrier and injectates. This system uses nitrogen gas for driving the mobile phase.

3.2.2 A Rheodyne injection valve, Model 7125 (USA), fitted with a 20  $\mu\text{L}$  stainless steel loop (0.5 mm i.d.) was employed for injection of all sulfur containing compounds.

3.2.3 A BAS flow cell, model cc5 (USA), was employed for the flow injection study. This model is channel flow. A boron-doped diamond thin-film was used as the working electrode, Ag/AgCl as the reference electrode and a stainless steel tube

on the outlet as the counter electrode. A neoprene gasket was used for controlling the space in the flow cell, in all experiments, the volume is 500  $\mu$ l.

3.2.4 A home-made flow cell, was employed to compare with the BAS flow cell.

3.2.5 A cutting set, Alltech.(USA) was used for cutting all plastic tube.

3.2.6 A PEEK tubing (0.25 mm i.d.) and connecting, Upchurch (USA), were used in this work.

3.2.7 A Teflon tubing (1/16" o.d.) Upchurch (USA), was used in this work.

### 3.3 Reagents

All chemicals used in this work were of analytical reagent grade and were obtained from various sources as shown in Table 3.1.

**Table 3.1** Listed of chemicals and suppliers.

| Chemical                                      | Formula                    | Supplier    |
|---|----------------------------|-------------|
| L-Cysteine                                    | $C_3H_7O_2NS$              | TCI (Japan) |
| DL-Homocysteine                               | $C_4H_9O_2NS$              | Sigma (USA) |
| Glutathione (GSH)                             | $C_{10}H_{17}O_6N_3S$      | Sigma (USA) |
| 2-Mercaptoethane sulfonic acid<br>Sodium salt | $C_2H_5O_3S_2.Na$          | Sigma (USA) |
| Cephalexin (Hydrate)                          | $C_{16}H_{17}O_4N_3S.H_2O$ | Sigma (USA) |
| Methionine                                    | $C_5H_{10}O_2NS$           | Sigma (USA) |
| Ampicilline                                   | $C_{16}H_{19}O_4N_3S$      | Sigma (USA) |

| Chemical                  | Formula                      | Supplier        |
|---------------------------|------------------------------|-----------------|
| Cystamine.dihydrochloride | $C_4H_{12}N_2S_2 \cdot 2HCl$ | Sigma (USA)     |
| Sodium Carbonate          | $Na_2CO_3$                   | Baker (Germany) |
| Sodium Hydrogen Carbonate | $NaHCO_3$                    | Merck (Germany) |
| Potassium Chloride        | KCl                          | Merck (Germany) |
| Potassium Hydroxide       | KOH                          | Merck (Germany) |
| Ethanol                   | $C_2H_6O$                    | Merck (Germany) |

### 3.4 The Preparation of Solutions

The preparation of solutions of sulfur-containing compounds and other solutions, employed in this work, are shown below. All solutions were prepared using deionized distilled water obtained from a Milli-Q system (Milford, MA, USA.)

#### 3.4.1 Carbonate buffer solutions

7.50 g of  $NaHCO_3$  and 1.70 g of  $Na_2CO_3$  were dissolved in 1.0 L of deionized water. The pH was adjusted to 9.2 using 0.1 M HCl and 0.1 M NaOH.

#### 3.4.2 Cysteine solutions

The 1.00 mM cysteine solution was prepared by weighing 0.0121 g cysteine crystal and transferring into 100 mL volumetric flask. The carbonate buffer solution was used for diluting this aliquot to the mark. This solution was used for investigating the oxidation of cysteine by cyclic voltammetry. The 50  $\mu$ M cysteine solutions for FIA study were prepared by measuring of 5 mL of 1.00 mM cysteine



solution into 100 mL volumetric flask. The carbonate buffer solution was used for diluting this aliquot to the mark.

#### 3.4.3 Homocysteine solutions

The 1.00 mM homocysteine solutions were prepared by weighing 0.0135 g homocysteine crystal and transferring into 100 mL volumetric flask. The carbonate buffer solution was used for diluting this aliquot to the mark. This solution was used for investigating of oxidation of homocysteine by cyclic voltammetry. The 50  $\mu$ M homocysteine solutions for FIA study were prepared by measuring 5 mL of 1.00 mM homocysteine solution by pipette and transferred into 100 mL volumetric flask. The carbonate buffer solution was used for diluting this aliquot to the mark.

#### 3.4.4 Glutathione solutions

The 1.00 mM glutathione solutions were prepared by weighing 0.0154 g glutathione powder and transferring into 100 mL volumetric flask. The carbonate buffer solution was used for diluting this aliquot to the mark. This solution was used for investigating of oxidation of glutathione by cyclic voltammetry.

#### 3.4.5 2-Mercaptoethane sulfonic acid solutions

The 1.00 mM 2-mercaptoethane sulfonic acid solutions were prepared by weighing 0.0164 g Na salt of 2-mercaptoethane sulfonic acid and transferring into 100 mL volumetric flask. The carbonate buffer solution was used for diluting this aliquot to the mark. This solution was used for investigating of oxidation of 2-mercaptoethane sulfonic acid by cyclic voltammetry. The 50  $\mu$ M 2-mercaptoethane sulfonic acid solutions for FIA study were prepared by measuring 5 mL of 1.00 mM 2-mercaptoethane sulfonic acid solution into 100 mL volumetric flask. The carbonate buffer solution was used for diluting this aliquot to the mark.

#### 3.4.6 Cephalexin solutions

The 10.0 mM cephalexin solutions were prepared by weighing 0.3654g cephalexin monohydrate powder and transferring into a 100 mL volumetric flask. The carbonate buffer solution was used for diluting this aliquot to the mark. This solution was used for investigating of the oxidation of cephalexin by cyclic voltammetry.

#### 3.4.7 Methionine solutions

The 1.00 mM methionine solutions were prepared by weighing 0.0149g methionine powder and transferring into a 100 mL volumetric flask. The carbonate buffer solution was used for diluting this aliquot to the mark. This solution was used for investigation of the oxidation of methionine by cyclic voltammetry.

#### 3.4.8 Cystamine solutions

The 1.00 mM cystamine solutions were prepared by weighing 0.0225g cystamine.dihydrochloride powder and transferring into a 100 mL volumetric flask. The carbonate buffer solution was used for diluting this aliquot to the mark. This solution was used for investigation of the oxidation of cystamine by cyclic voltammetry.

#### 3.4.9 Ampicillin solutions

The 1.00 mM ampicillin solutions were prepared by weighing 0.0349g ampicillin powder and transferring into a 100 mL volumetric flask. The carbonate buffer solution was used for diluting this aliquot to the mark. This solution was used for investigation of the oxidation of ampicillin by cyclic voltammetry.

### 3.5 Procedure

#### 3.5.1 The Oxidation of Sulfur-Containing Compounds

In all cyclic voltammetric studies, a boron-doped diamond thin-film was used as the working electrode, the results of which were compared with those from a glassy carbon electrode. An Ag/AgCl was employed as the reference electrode and a platinum wire was employed as the counter electrode.

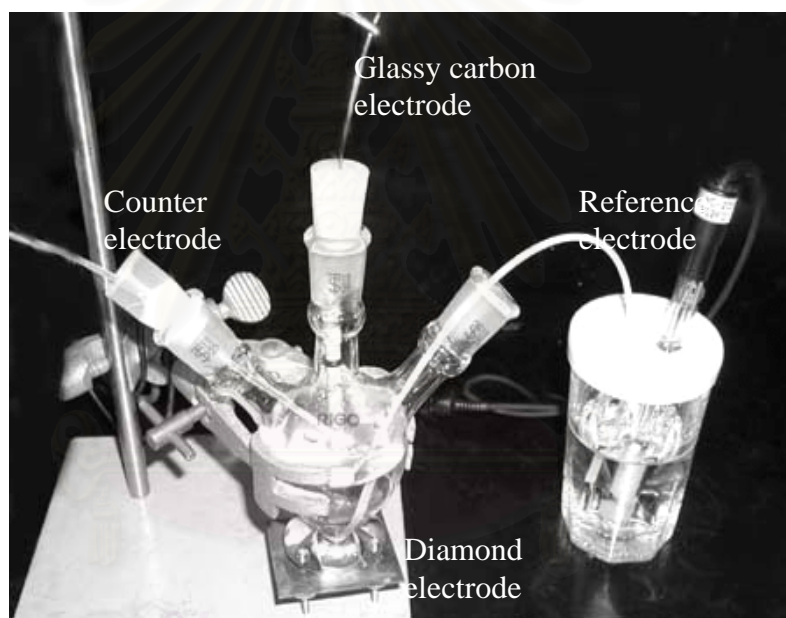


Figure 3.2 The electrochemical cell for cyclic voltammetric study

### 3.5.1.1 pH dependence

This experiment was done for optimizing pH conditions for other experiments. Cysteine was used as a model in this study. 1.0 mM cysteine solutions were prepared in pH 6, 8 and 10 phosphate buffer, respectively. These solutions were studied by cyclic voltammetry.

### 3.5.1.2 The anodic potential of sulfur-containing compounds

Using the chosen buffer solution from the prior experiment and 1.0 mM sulfur-containing compound solutions in carbonate buffer pH 9.2, the oxidation on the electrode surface was studied at a scan rate 50 mV/s from potential range of 0 to 1.1 V.

### 3.5.1.3 The scan rate dependence study

The solutions of 1.0 mM sulfur-containing compound solutions in carbonate buffer pH 9.2 were studied at various scan rate to find adsorption of these compounds on the surface of electrode. The scan rates used in these experiments were 10, 20, 50, 100, 200 and 500 mV/s.

### 3.5.1.4 The concentration dependence study

In each scan rate, 0.1, 0.5, 1.0, 2.0, 5.0 and 10 mM sulfur-containing compound solutions in carbonate buffer pH 9.2 were studied and the calibration curve was constructed using these voltammetric data.

### 3.5.2 The Home-made Flow Cell

The thin layer home-made flow cell was built. Polyacrylonitrile plates were used as a body of cell show as Figure 3.3. The diameter of inlet and outlet is 1.3 mm. The salt-bridge of the reference electrode was connected between the inlet and the outlet. The 1/16" o.d. stainless steel tube, outlet, was used as a counter electrode. The working electrode area and volume in cell were controlled by a neoprene gasket. The gasket's volume was 500  $\mu\text{L}$ .

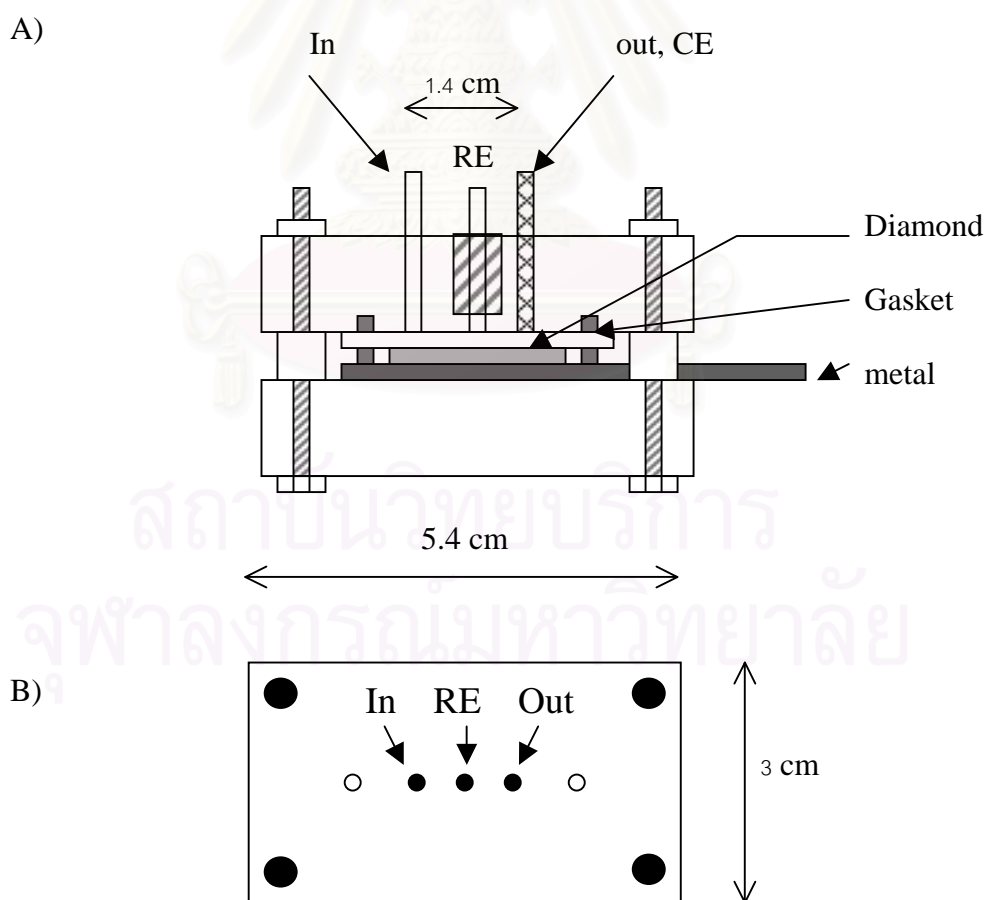


Figure 3.3 The modified flow cell: (A) a side view of cell and (B) a plan view

### 3.5.3 The Optimization of the FI System

The sulfur-containing compounds were studied using a flow injection system with amperometric detection. Boron-doped diamond thin-film was employed as the working electrode. Ag/AgCl was employed as the reference electrode and platinum tube was employed as the counter electrode. BAS flow cell was used in this experiment. 0.1 M Carbonate buffer pH 9.2 was used as the carrier in all studies. A flow rate of the mobile phase was 1.0 mL/min. The schematic diagram of the FI system was shown in Figure 3.4

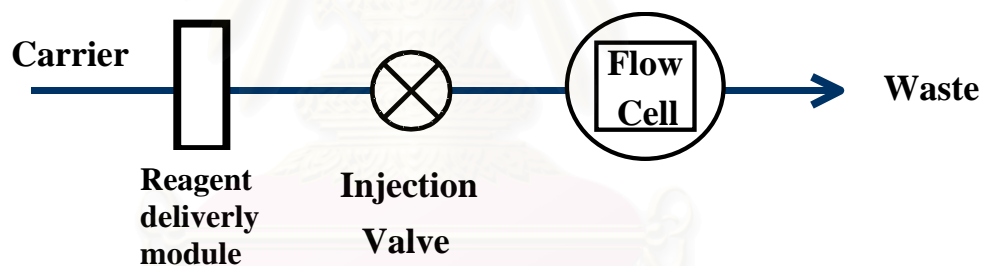


Figure 3.4 The schematic diagram of FI system

#### 3.5.3.1 Hydrodynamic measurement

50  $\mu\text{M}$  sulfur-containing compound in 0.1 M carbonate buffer pH 9.2 was injected while the potentials at the boron-doped diamond thin-film were held at 0, 0.2, 0.4, 0.5, 0.6, 0.7, 0.8, 0.9 and 1.0 V. The hydrodynamic curve ( $E$  vs.  $i$ ) from the acquired data would show the optimum voltage for detection.

### **3.5.4 Repeatability**

This study was carried out under the optimal conditions of the FI system. The repeatability of FI was determined using 50  $\mu\text{M}$  sulfur-containing compound solutions. The sulfur-containing compound solution was injected fifty times. Results obtained were used in calculating the relative standard deviation (RSD).

### **3.5.5 Detection Limit**

For cyclic voltammetry, the limit of detection (LOD) was determined. The LOD was defined as the lowest peak current after subtracts background.

For FIA, this study was carried out under the optimal conditions of the FI system. The LOD was defined as three times the signal to noise ratio.

### **3.5.6 Comparison with the Other Flow Cell**

The home-made flow cell was compared with the BAS flow cell for the analysis of 2-mercaptoethane sulfonic acid. The repeatability and the detection limit of the cell were studied. The optimal condition had been established.



## CHAPTER IV

### RESULTS AND DISCUSSION

#### 4.1 The Oxidation of Sulfur Containing Compounds

##### 4.1.1 pH Dependence

For redox reaction of organic compounds, the peak position and the shape of the voltamogram depend on the pH of the buffer. Therefore, pH controlling is very important. Various types of material used to make electrodes are also critical because they limit the working pH range. Boron-doped diamond thin-film is a durable material, which can be used over a wide range of pH values. In this experiment, cysteine was used as a model for sulfur-containing compounds to find a suitable pH for the boron-doped diamond thin-film electrode for all measurements.

In this experiment, the actual pH of solution was measured after dissolving cysteine because cysteine was an acidic compound and the pH of solution decreased after dissolution cysteine. In the potential window from 0 to 1.1 V, an anodic peak current was not observed when the buffer solution of pH 4 was used, it indicates that the oxidation may occur at a potential higher than 1.1 V. The peak potential of cysteine at various pH values, shown in Table 4.1, indicates that the oxidation potential increases when the pH decreases. The data show that oxidation of sulfur-containing compounds occurs easily at basic pH.

Table 4.1 The oxidation potentials of cysteine at various pH

|            | pH  |      |      |      |
|------------|-----|------|------|------|
|            | 4.0 | 6.2  | 8.0  | 10   |
| $E_{pa}^*$ | x   | 0.97 | 0.81 | 0.63 |

\* In potential window 0 to 1.1 V, x is no observed peak

A solution of 0.1 M carbonate buffer pH 9.2 was chosen because the electrode surface was easily damaged in strong basic alkali solution. So, we chose carbonate buffer as a buffer for all measurement.

#### 4.1.2 The Anodic Potential of Sulfur-Containing Compounds

The background current of carbonate buffer pH 9.2 was studied with cyclic voltammetry. At low potentials, the background current received from the boron-doped diamond thin-film electrode was low (Figure 4.1), however when the potential was moved positive, the current was higher. Glassy carbon showed a low background current but it was higher than the one received from the boron-doped diamond thin-film electrode (Figure 4.2). Therefore, the potential window from 0 to 1.1 V was used for all of next experiments.

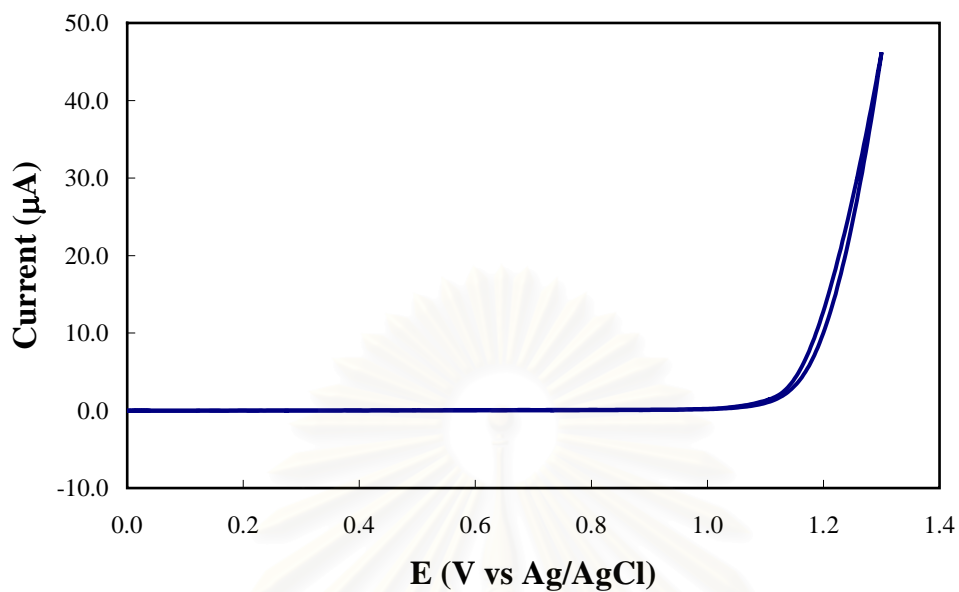


Figure 4.1 Cyclic voltammogram of 0.1 M carbonate buffer pH 9.2, using boron-doped diamond thin-film electrode at scan rate 0.05 V/s from 0 to 1.3 V vs. Ag/AgCl. The area of electrode is 0.07 cm<sup>2</sup>.

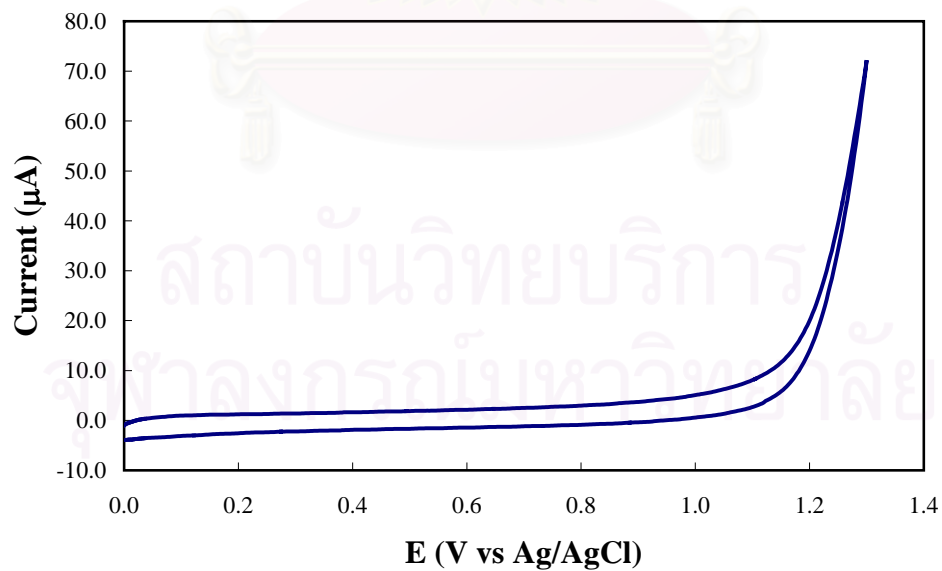


Figure 4.2 Cyclic voltammogram of 0.1 M carbonate buffer pH 9.2, using glassy carbon electrode at scan rate 0.05 V/s from 0 to 1.3 V vs. Ag/AgCl. The area of electrode is 0.07 cm<sup>2</sup>.

The solution of 0.1 M carbonate buffer pH 9.2 was used with a scan rate of 0.05 V/s and a potential window from 0 to 1.1 V. Sulfur-containing compounds selected for study were cysteine, homocysteine, methionine, glutathione, 2-mercaptoethane sulfonic acid, cephalixin and ampicillin. With the solution of 0.1M carbonate buffer pH 9.2, scan rate 0.05 V/s and a potential range from 0 to 1.1 V, well-defined peaks for cysteine, homocysteine, glutathione, 2-mercaptoethane sulfonic acid and cephalixin were observed (Figures 4.3 and 4.4). However the oxidation peak of methionine, ampicillin and cystamine did not occur in the potential range from 0 to 1.1 V (Figure 4.5). We tried to run cyclic voltammograms of methionine at higher potentials up to 1.3 V. There was no observed peak for ampicillin and methionine but we observed a poorly define peak for cystamine (Figure 4.6A). Searching for peak position of cystamine was difficult due to the poor peak shape, and it was necessary to subtract the background signal (Figure 4.6B) for correcting the cystamine signal. The cystamine signal after background signal substration is shown in figure 4.6C.

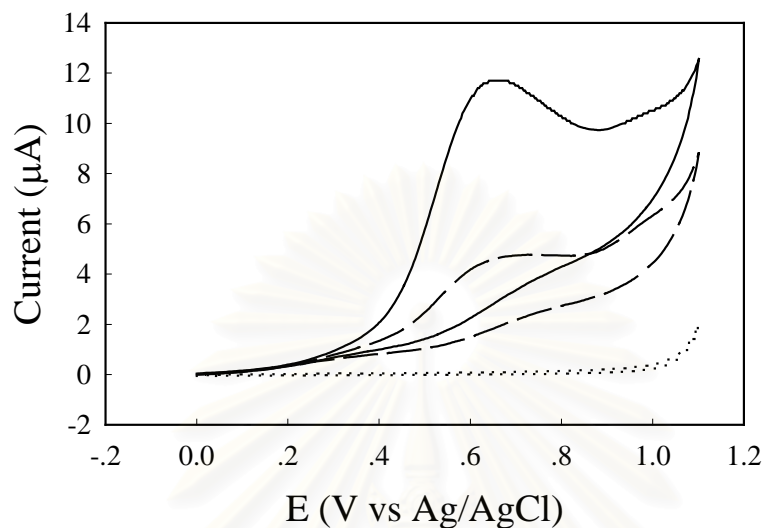


Figure 4.3 Cyclic voltammogram of 1.0 mM cysteine in 0.1 M carbonate buffer pH 9.2 using boron-doped diamond thin-film electrode at scan rate of 0.05 V/s from 0 to 1.1 V vs. Ag/AgCl., the area of electrode of 0.07 cm<sup>2</sup>. (—) first scan, (---) second scan and (···) background.

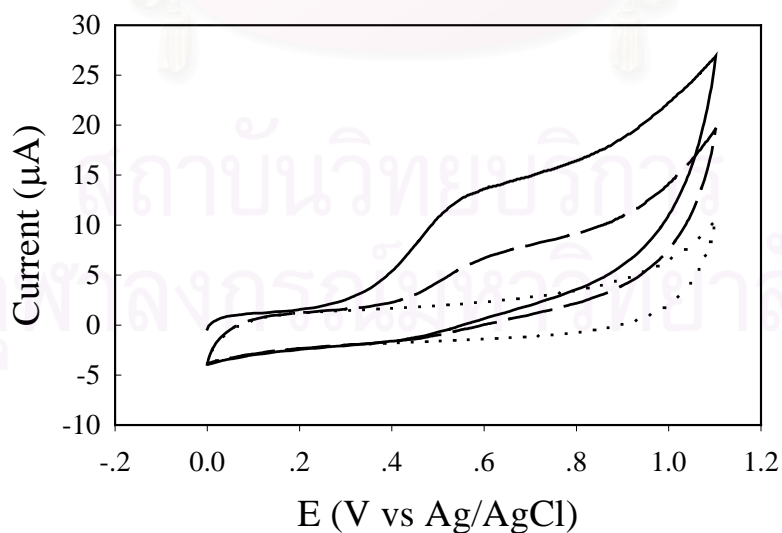


Figure 4.4 Cyclic voltammogram of 1.0 mM cysteine in 0.1 M carbonate buffer pH 9.2 using glassy carbon electrode at scan rate of 0.05 V/s from 0 to 1.1 V vs.

Ag/AgCl., the area of electrode of  $0.07 \text{ cm}^2$ . (—) first scan, (---) second scan and (....) background.

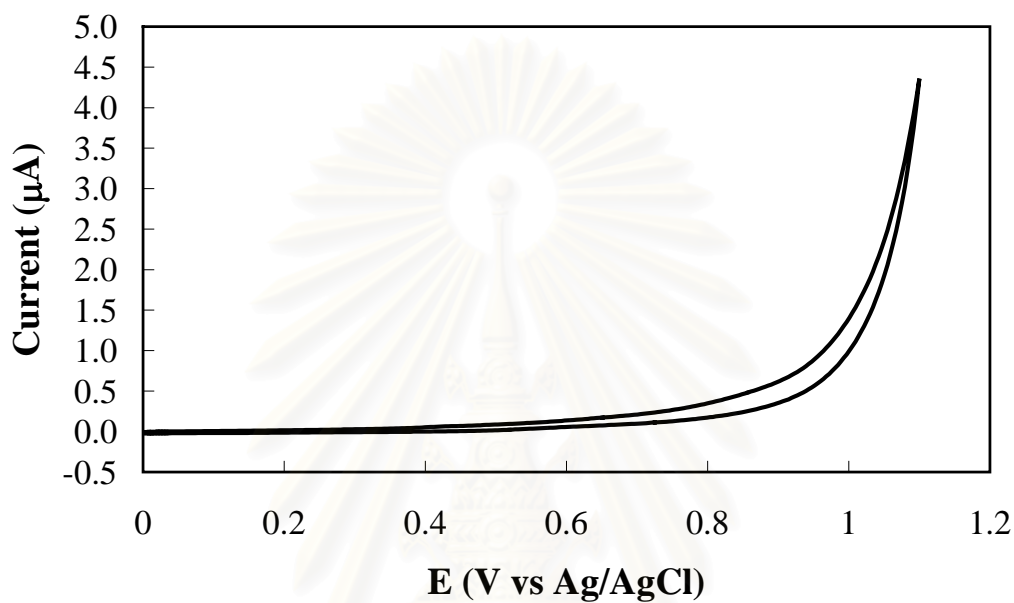


Figure 4.5 Cyclic voltammogram of 1.0 mM ampicillin in 0.1 M carbonate buffer pH 9.2 using glassy carbon electrode at scan rate of 0.05 V/s from 0 to 1.1 V vs.

Ag/AgCl., the electrode area of  $0.07 \text{ cm}^2$ .

สถาบันวิทยบริการ  
จุฬาลงกรณ์มหาวิทยาลัย

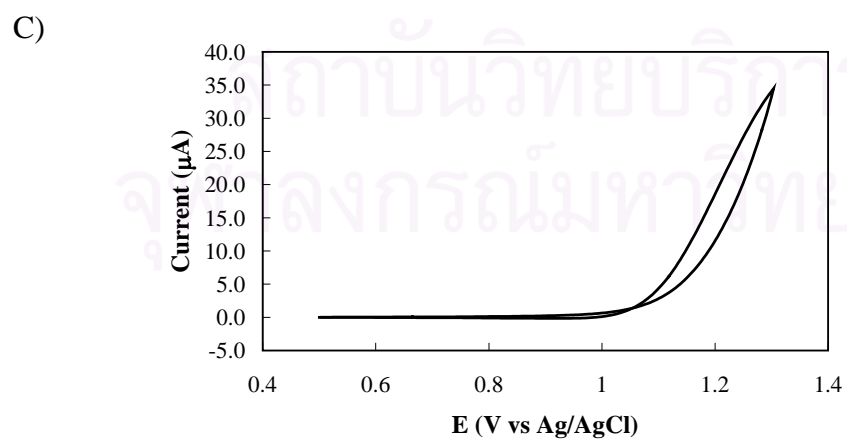
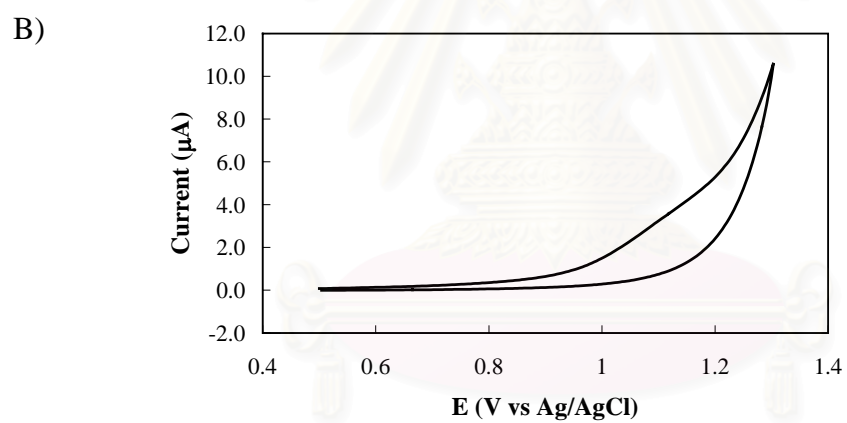
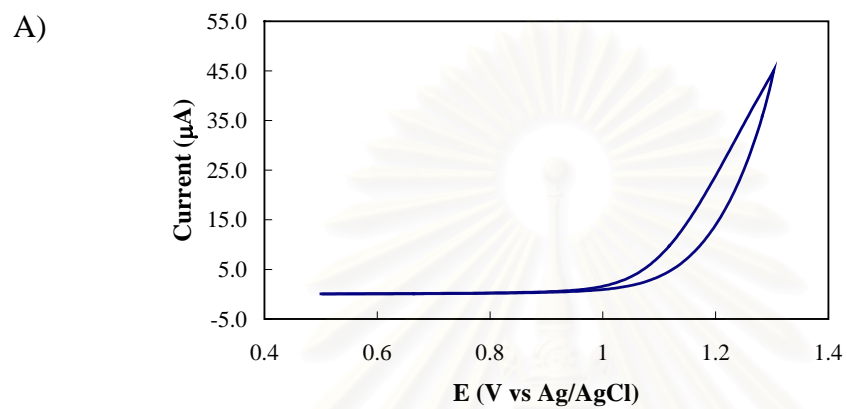




Figure 4.6 Cyclic voltammogram of (A) 1.0 mM cystamine in 0.1 M carbonate buffer pH 9.2, (B) carbonate buffer pH 9.2 using boron-doped diamond thin-film electrode at scan rate of 0.05 V/s from 0.5 to 1.3 V vs. Ag/AgCl., the electrode area of 0.07 cm<sup>2</sup> and (C) subtracted voltammogram of (A) and (B).

Table 4.2 The peak potential and anodic peak current of 1.0 mM sulfur-containing compounds from cyclic voltammetry at scan rate of 0.05 V/s, electrode area of 0.07 cm<sup>2</sup>

| Sulfur containing compounds   | Diamond electrode     |       | Glassy carbon electrode |       |
|-------------------------------|-----------------------|-------|-------------------------|-------|
|                               | E <sub>peak</sub> (V) | I(μA) | E <sub>peak</sub> (V)   | I(μA) |
| Cysteine                      | 0.638                 | 8.508 | 0.568                   | 5.763 |
| Homocysteine                  | 0.629                 | 2.858 | 0.586                   | 1.152 |
| Glutathione                   | 0.674                 | 8.327 | -                       | -     |
| 2-Mercaptoethanesulfonic acid | 0.527                 | 10.35 | 0.795                   | 3.640 |
| Cephalexin*                   | 0.577                 | 1.589 | 0.593                   | 1.142 |
| Methionine                    | -                     | -     | -                       | -     |
| Ampicillin                    | -                     | -     | -                       | -     |
| Cystamine                     | 1.270                 | 3.020 | -                       | -     |

\* The concentration of Cephalexin is 10.057 mM and - is no observed peak

The cyclic voltammograms of cysteine, homocysteine, glutathione, 2-mercaptoethane sulfonic acid and cephalexin obtained at the boron-doped diamond thin-film electrode exhibited better-defined peaks than those from the glassy carbon

electrode. Peak shape determines the accuracy of the peak position and current measurement. The peak potential and anodic peak current of sulfur-containing compounds are shown in Table 4.2. Boron-doped diamond thin-film electrode was an excellent electrode for detecting sulfur-containing compound and it was better than the glassy carbon electrode. The oxidation of cysteine, homocysteine, glutathione, 2-mercaptoethane sulfonic acid and cephalixin occurred at 0.638, 0.629, 0.674, 0.527 and 0.577 V, respectively. The oxidation of cystamine occurred at very high potential (1.270 V). Even though the boron-doped diamond thin-film is a durable and inert material, the long term stability of this electrode will decrease when it was used at high potential. The scan rate and concentration dependence of cysteine, homocysteine, glutathione, 2-mercaptoethane sulfonic acid and cephalixin were studied.

Using cyclic voltammograms at both electrodes, it was found that the anodic currents from second scan were lower than those of the first scan. The explanation for these results is that following the oxidation product of sulfur-containing compounds is normally a dimer obtained via a sulfur radical [12]:



The products covers the surface of the electrode and obstructs the diffusion of any compound to the electrode surface. However, the layer product films do not permanently adsorb on an the electrode surface, they could be removed by blowing water over the surface. This allows the anodic current to recover. From this fact, flow injection analysis would overcome the fouling problem. Therefore, flow

injection analysis of sulfur-containing compounds was studied with electrochemical detection (Section 4.2).

According to Table 4.2, the anodic potentials depend on the structures of sulfur compound (Figure 4.7). Four of them are thiols and the other is a thioether. The results of the four thiols showed that the smaller and less sterically hindered molecules had lower anodic potentials. The oxidation may occur via a radical because cysteine has a higher potential than 2-mercaptoethane sulfonic acid. The sulfonic group is a better receiving group than the amine or carboxylic groups and it could stabilize the S-radical in intermediate steps. In this way, cephalixin has a lower anodic potential than the other three amino acids because the cyclic structure of cephalixin can stabilize its intermediate.



สถาบันวิทยบริการ  
จุฬาลงกรณ์มหาวิทยาลัย

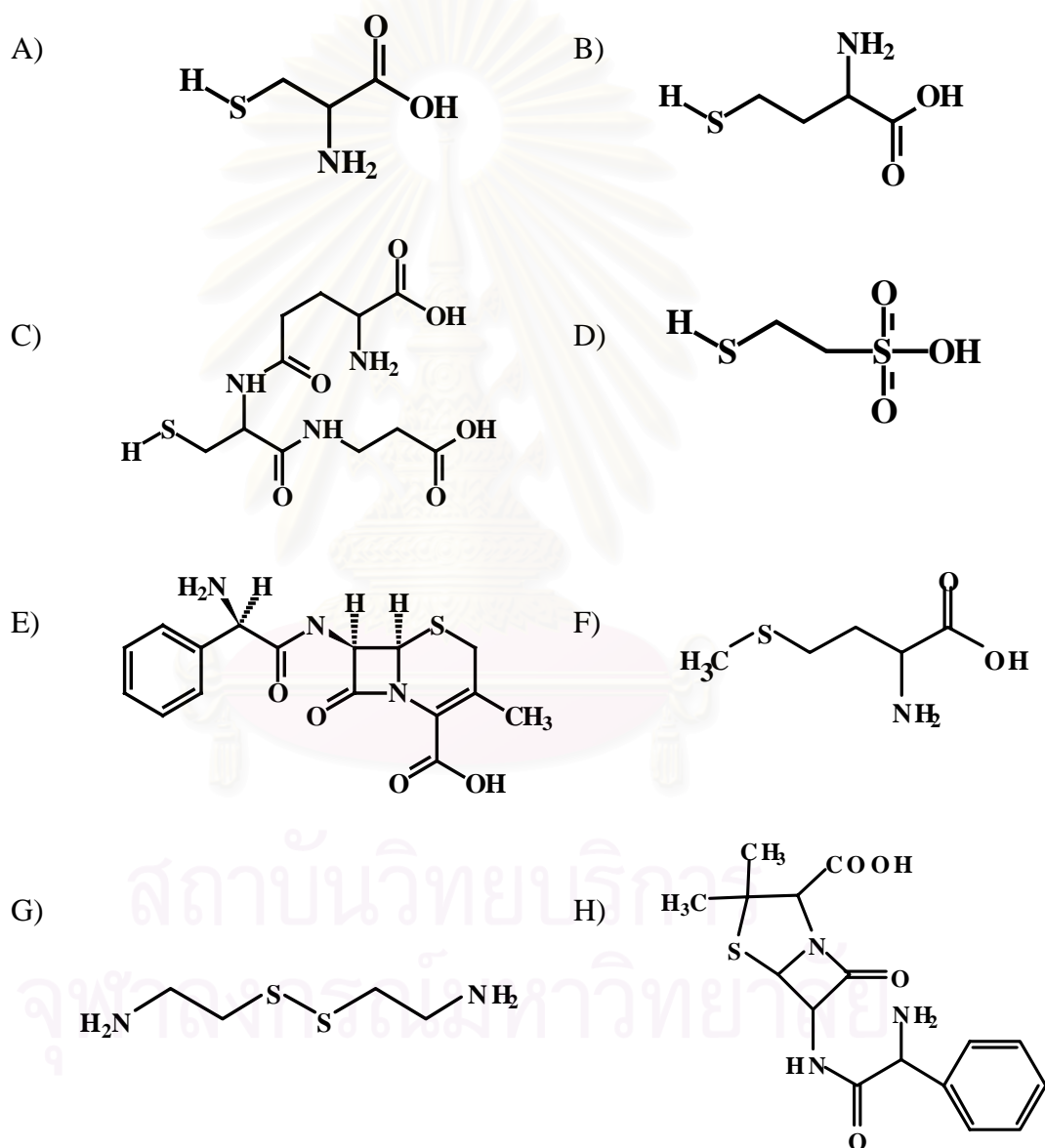


Figure 4.7 Structures of sulfure-containing compounds: (A) cysteine, (B) homocysteine, (C) glutathione, (D) 2-mercaptoethane sulfonic acid and

(E) cephalixin, (F) methionine, (G) cystamine and (H) ampicillin

There is a prediction that the oxidation peak obtained from the oxidation of the sulfur group. It is not the oxidation of the amino group because it has been reported that the oxidation of amine compounds with diamond electrode in carbonate buffer pH 10 occurs at the higher potentials than 0.9 V [13].

#### 4.1.3 The Scan Rate Dependence Study

When scan rates were varied, the anodic potential changed for all sulfur-containing compounds, for example, cephalixin (Figure 4.8) because the oxidation of sulfur-containing compounds is an irreversible reaction. The higher scan rate used, the higher the anodic current obtained. For totally irreversible reactions the Nernstian boundary condition is replaced by [14]

$$\frac{i}{nFA} = D_o \left[ \frac{\partial C_o(x,t)}{\partial x} \right]_{x=0} = k_f(t) C_o(0,t) \quad (4.1)$$

when

$i$  = current (A)

$n$  = electrons per molecule oxidized; faradays per mole of

substance electrolyzed

$F$  = the faraday; charge on one mole of electrons (C)

$A$  = area (cm<sup>2</sup>)

$D_o$  = diffusion coefficient of species  $o$  (cm<sup>2</sup>/sec)

$C_o(x,t)$  = concentration of species  $o$  at the distance  $x$  at time  $t$

$k_f$  = heterogeneous rate constant for “forward” reaction

The current is given by

$$i = nFAC_o^*Do^{1/2}v^{1/2}\left(\frac{\alpha n_a F}{RT}\right)^{1/2} \pi^{1/2} \chi(bt) \quad (4.2)$$

Where  $\chi(bt)$  is a tabulated function. From equation (4.2), it shows  $i$  at any point on the wave depend on  $v^{1/2}$  and  $C_o^*$ .

When

$C_o^*$  = bulk concentration of species  $o$

$\alpha$  = transfer coefficient

$n_a$  = number of electrons involved in the rate-determining step

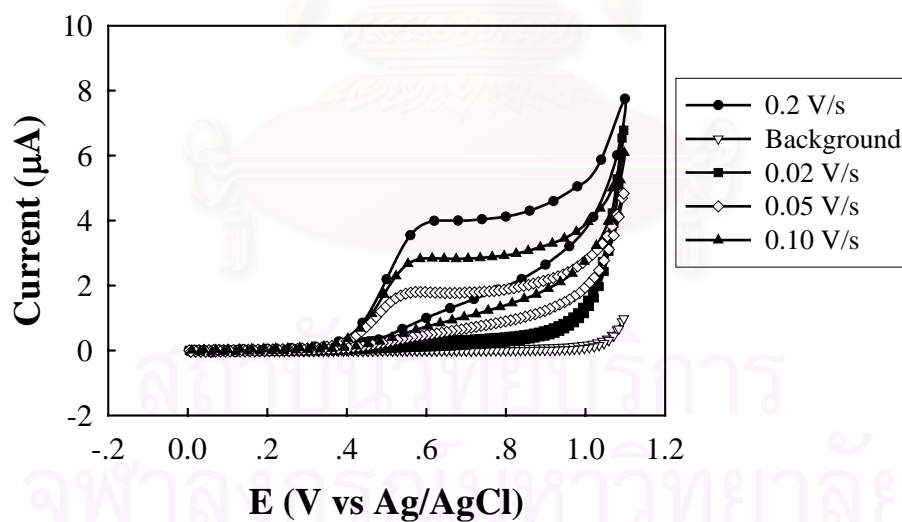


Figure 4.8 Cyclic voltammogram of 10.0 mM cephalixin in 0.1 M carbonate buffer pH 9.2 using boron-doped diamond thin-film electrode, potential range from 0 to 1.1 V vs. Ag/AgCl. The area of electrode is  $0.07 \text{ cm}^2$ : (●) scan rate 0.20 V/s, (◇) scan rate 0.10 V/s, (▲) scan rate 0.05 V/s, (■) scan rate 0.02 V/s and

(—▽—) background current at scan rate 0.05 V/s

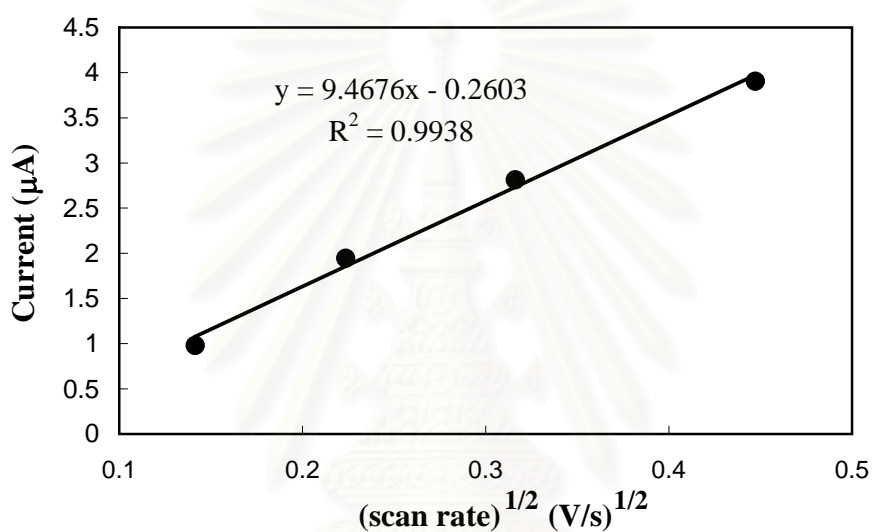


Figure 4.9 (scan rate)<sup>1/2</sup> vs current of 10.0 mM cephalixin in 0.1 M carbonate buffer pH 9.2 using boron-doped diamond thin-film electrode. The area of electrode is 0.07 cm<sup>2</sup>.

As shown in Figure 4.9, there is a linear relationship between (scan rate)<sup>1/2</sup> and current (correlation coefficient is 0.9938). This indicates that the oxidation of sulfur-containing compounds is an irreversible reaction and sulfur-containing compounds do not adsorb on diamond electrode surface.



#### 4.1.4 The Concentration Dependence Study

The concentration dependence was determined for sulfur-containing compounds on boron-doped diamond thin-film and glassy carbon electrodes. The response was higher and more linear for the boron-doped diamond electrode. Figure 4.10 shows a series of cyclic voltammograms obtained at a sweep rate 100 mV/s for various homocysteine concentrations for a boron-doped diamond electrode (and as Figure 4.11 for a glassy carbon electrode). For an irreversible reaction, such as sulfur compounds oxidation, the anodic potential will shift with a change in the concentration of the electroactive species. For calibration curve for the boron-doped diamond electrode, the voltammetric response was almost perfectly linear, while that for glassy carbon electrode was not (Figure 4.12). A slope indicated sensitivity of electrode for each sulfur compounds. The slope for boron-doped diamond calibration curve was a factor of 1.80 greater than that for glassy carbon electrode. The other sulfur-containing compounds were examined and results are shown in Table 4.3.

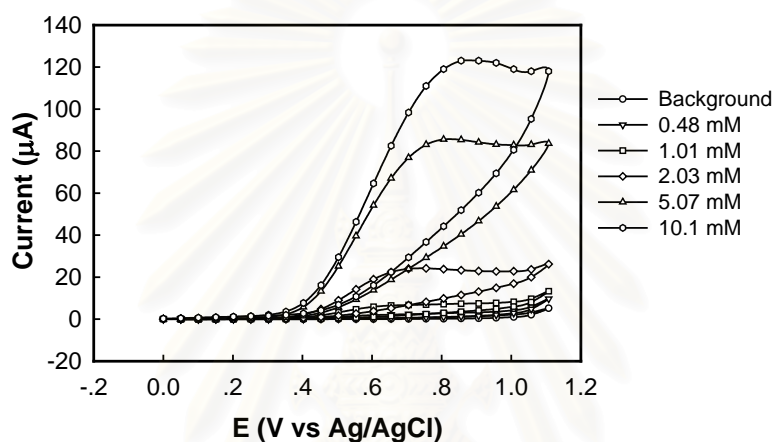


Figure 4.10 Cyclic voltammograms for boron-doped diamond thin-film electrode in pH 9.2 carbonate buffer for a series of homocysteine concentration: 0, 0.48, 1.01, 1.03, 50.7 and 10.1 mM. Potential sweep rate, 100 mV/s; electrode area of 0.07 cm<sup>2</sup>.

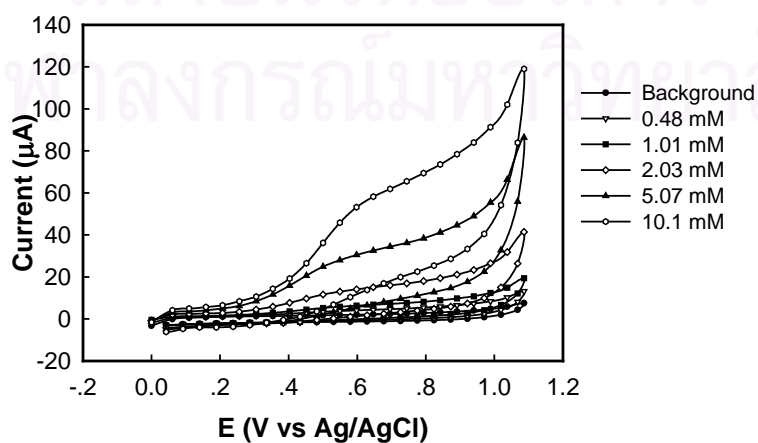


Figure 4.11 Cyclic voltammograms for glassy carbon electrode in pH 9.2 carbonate buffer for a series of homocysteine concentration: 0, 0.48, 1.01, 1.03, 50.7 and 10.1 mM. Potential sweep rate, 100 mV/s; electrode area of 0.07 cm<sup>2</sup>.

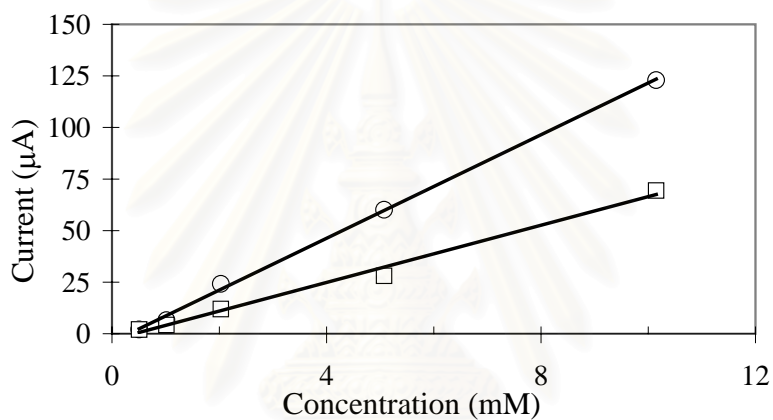


Figure 4.12 The calibration curves of homocysteine in 0.1 M carbonate buffer, pH 9.2 using (○) boron-doped diamond thin-film and (□) glassy carbon electrodes. Potential sweep rate, 100 mV/s; electrode area, 0.07 cm<sup>2</sup>. The correlation coefficients are 0.9988 and 0.9922, respectively.

Table 4.3 Sensitivity, linear range and limit of detection of sulfur-containing compounds for boron-doped diamond thin-film and glassy carbon electrodes using cyclic voltammetry.

|                                | Diamond      |                |              |         | Glassy carbon |                |              |         |
|--------------------------------|--------------|----------------|--------------|---------|---------------|----------------|--------------|---------|
|                                | Sensitivity* | R <sup>2</sup> | Linear range | LOD(mM) | Sensitivity*  | R <sup>2</sup> | Linear range | LOD(mM) |
| Cysteine                       | 12.40        | 0.9994         | 0.5mM-10mM   | 0.5     | 5.17          | 0.9977         | 0.5mM-10mM   | 0.5     |
| Homocysteine                   | 12.56        | 0.9988         | 0.5mM-10mM   | 0.5     | 6.94          | 0.9922         | 0.5mM-10mM   | 0.5     |
| Glutathione                    | 12.49        | 0.9965         | 0.5mM-10mM   | 0.5     | -             | 0.9930         | -            | -       |
| 2-Mercaptoethane sulfonic acid | 10.35        | 0.9991         | 0.5mM-10mM   | 0.5     | 7.44          | 0.9987         | 0.5mM-10mM   | 0.5     |
| Cephalexin                     | 0.159        | 0.9959         | 10mM-25mM    | 10      | 0.154         | 0.9937         | 10mM-25mM    | 10      |

## 4.2 The Home-made Flow Cell

A thin layer flow cell according to the plan shown in Figure 4.13 was built. The completed flow cell is shown in Figure 4.14. The performance of this flow cell are discussed in Section 4.6.

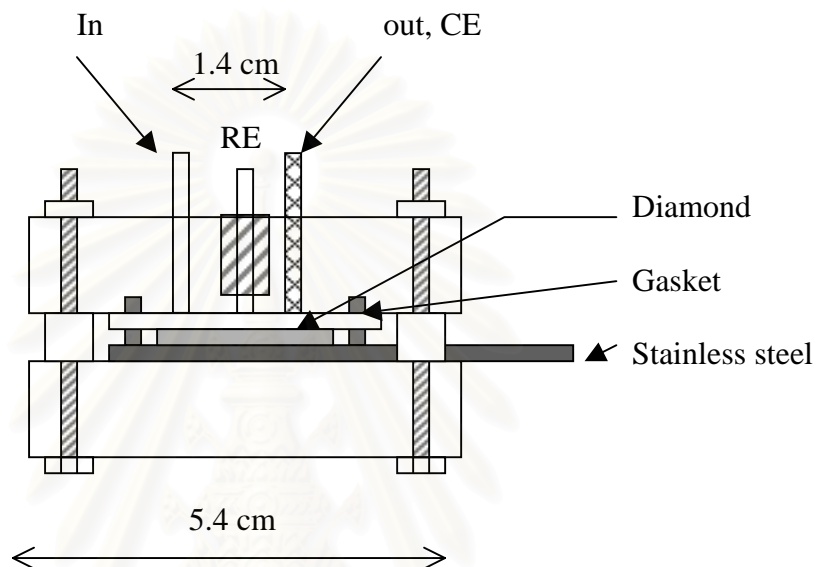


Figure 4.13 The modified flow cell.

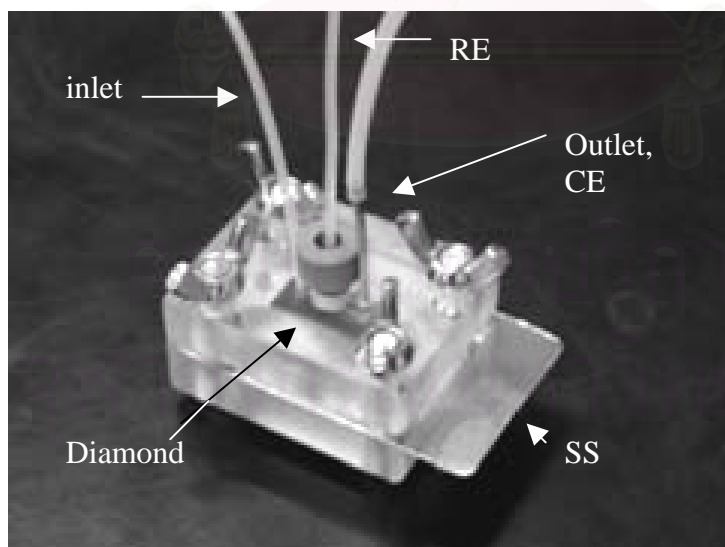


Figure 4.14 The completed home-made flow cell

### 4.3 The optimization of the FI system

Three sulfur-containing compounds: cysteine, homocysteine and 2-mercaptoethane sulfonic acid was chosen for study in this section because they provided high sensitivities at the boron-doped diamond thin-film electrode.

#### 4.3.1 Hydrodynamic measurement

##### 4.3.1.1 The solution of 0.1 M carbonate buffer pH 9.2.

At first the hydrodynamics of the carrier (The solution of 0.1 M carbonate buffer, pH 9.2) or hydrodynamic background were studied. Figure 4.14 shows the background hydrodynamic  $i$ - $E$  curve at the boron-doped diamond thin-film electrode in 0.1 M carbonate buffer, pH 9.2. The carrier flow rate was 1.0 mL/min. Each datum was recorded at the end of a 2 min period at each applied potential. As the potentials range from 0 to 0.9, the current response range is 10 to 100 nA. The anodic current increased dramatically from 100 to 550 nA when the positive potential changed from 0.9 to 1.0 V.

สถาบันวิทยบริการ  
จุฬาลงกรณ์มหาวิทยาลัย

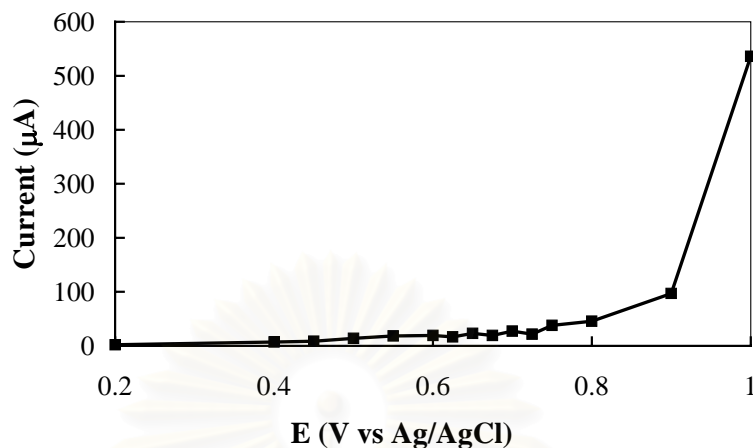


Figure 4.15 Background hydrodynamic  $i$ - $E$  curve at the boron-doped diamond thin-film electrode in 0.1 M carbonate buffer, pH 9.2. Flow rate 1.0 mL/min. Each datum was recorded at the end of a 2 min period of holding potential.

#### 4.3.1.2 Cysteine

After obtaining the background hydrodynamic curve, the hydrodynamics were studied of the sulfur-containing compounds. Figure 4.16 shows the hydrodynamic  $i$ - $E$  curve at the boron-doped diamond thin-film electrode during 20- $\mu$ L injections of 50  $\mu$ M cysteine in 0.1 M carbonate buffer, pH 9.2. The carrier flow rate was 1.0 mL/min. Each datum represents the average of 10 injections. The well-defined sigmoidal curve is shown in Figure 4.16. The hydrodynamic  $i$ - $E$  curve for cysteine was shifted positive from its potential in the linear voltammogram. This shift was caused by resistance effects within the flow cell. The potential chosen as an optimized potential for the quantitative study of cysteine in the FI system was 0.55 V.



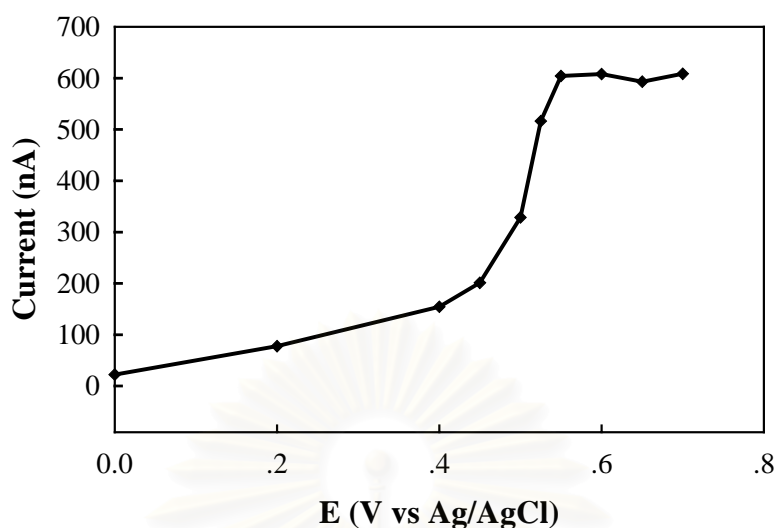


Figure 4.16 Hydrodynamic  $i$ - $E$  curve at the boron-doped diamond thin-film electrode exposed to 20- $\mu$ L injection of 50  $\mu$ M cysteine in 0.1 M carbonate buffer, pH 9.2. Flow rate 1.0 mL/min. Each datum represents the average of 10 injections.

#### 4.3.1.3 Homocysteine

Unlike cysteine, the hydrodynamic  $i$ - $E$  curve of homocysteine was not a well-defined sigmoidal curve (Figure 4.17). It was difficult to define an optimized potential for this FI system. Generally, the ratio between the hydrodynamic signal of the sample and the background signal will be used. Figure 4.18 shows the corrected  $i$ - $E$  curve for the hydrodynamic 20- $\mu$ L injection of 50  $\mu$ M homocysteine in 0.1 M carbonate buffer, pH 9.2. The carrier flow rate was 1.0 mL/min. Each datum represents the average of 10 injections. The potential we chose as an optimized potential for detecting homocysteine in the FI system was 0.775 V.

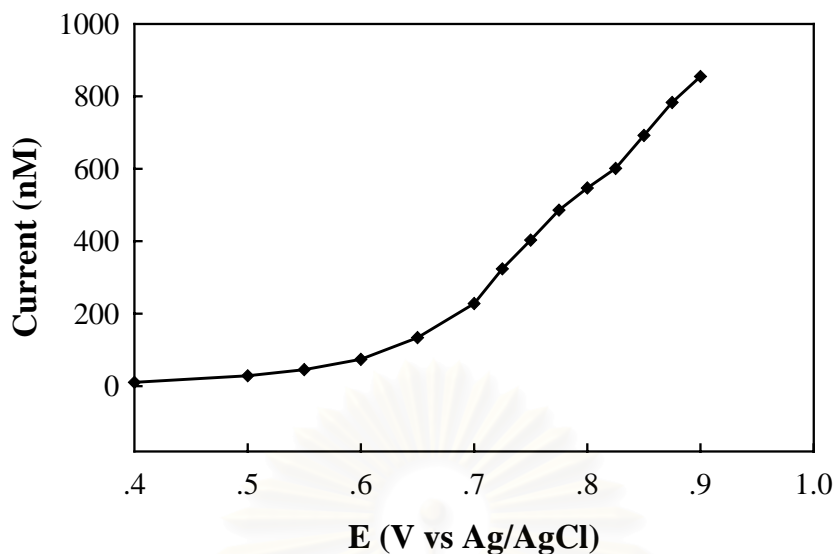


Figure 4.17 Hydrodynamic  $i$ - $E$  curve at the boron-doped diamond thin-film electrode exposed to 20- $\mu$ L injection of 50  $\mu$ M homocysteine in 0.1 M carbonate buffer, pH 9.2. Flow rate 1.0 mL/min. Each datum represents the average of 10 injections.

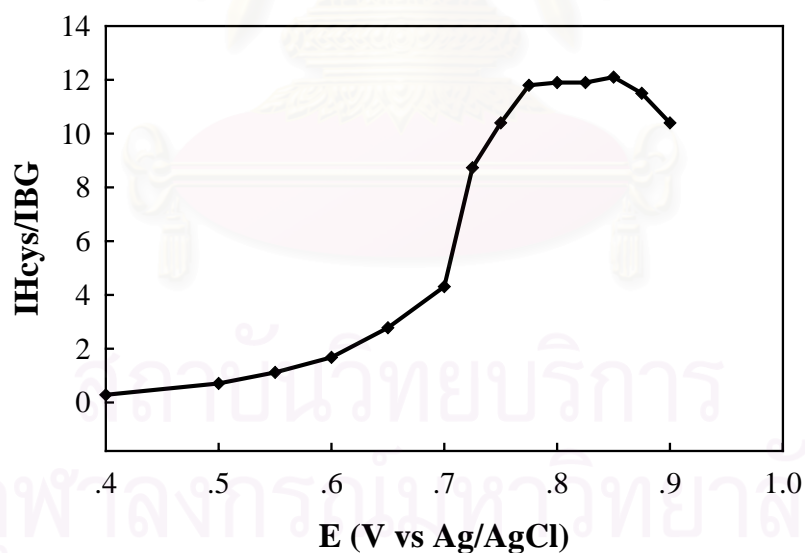


Figure 4.18 Hydrodynamic after correcting background at the boron-doped diamond thin-film electrode exposed to 20- $\mu$ L injection of 50  $\mu$ M homocysteine in 0.1 M carbonate buffer, pH 9.2. Flow rate 1.0 mL/min. Each datum represents the average of 10 injections.

#### 4.3.1.4 2-Mercaptoethane sulfonic acid

Similar to homocysteine, the hydrodynamic  $i$ - $E$  curve of 2-mercaptoethane sulfonic acid was not a well-defined sigmoidal curve. The hydrodynamic signal of 2-mercaptoethane sulfonic acid was corrected by dividing by the background signal. The correct hydrodynamic for boron-doped diamond thin-film electrode exposed to 20- $\mu$ L injection of 50  $\mu$ M homocysteine in 0.1 M carbonate buffer, pH 9.2 is shown in Figure 4.19. The carrier flow rate was 1.0 mL/min. Each datum represents the average of 10 injections. The potential, which was chosen as an optimized potential for the detection of 2-mercaptoethane sulfonic acid in FI system, was 0.625 V.

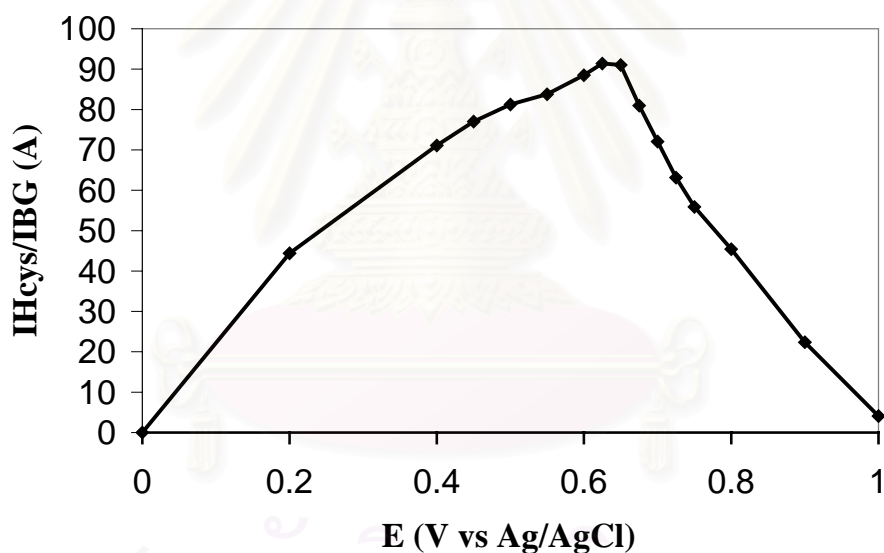
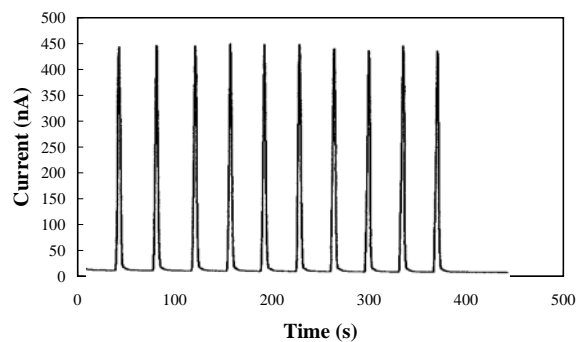


Figure 4.19 Hydrodynamic after correcting background at the boron-doped diamond thin-film electrode exposed to 20- $\mu$ L injection of 50  $\mu$ M 2-mercaptoethane sulfonic acid in 0.1 M carbonate buffer, pH 9.2. Flow rate 1.0 mL/min. Each datum represents the average of 10 injections.

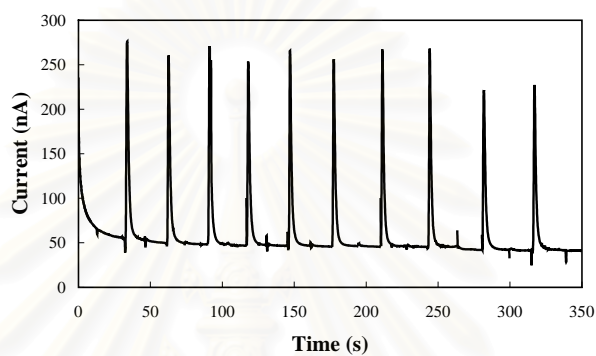
#### 4.4 Repeatability

The repeatabilities were studied by injecting fifty 20- $\mu$ L of 50  $\mu$ M of sulfur-containing compounds in 0.1 M carbonate buffer, pH 9.2. The detection potential obtained from the hydrodynamic curve in Section 4.3. Figure 4.20 shows the response of the boron-doped diamond thin-film, to 50 injections of (A) 50  $\mu$ M cysteine, (B) 50  $\mu$ M homocysteine and (C) 50  $\mu$ M 2-mercaptoethane sulfonic acid in 0.1 M carbonate buffer, pH 9.2. The mobile phase flow rate was 1.0 mL/min and the dc potentials were 0.55, 0.775 and 0.625, respectively. The reproducibilities were obtained as the coefficient of variation (%RSD) in the peak height (current). The peaks of cysteine, homocysteine and 2-mercaptoethane sulfonic acid were sharp and narrow with width at half-height of 2, 3 and 2.5 s.

A)



B)



C)

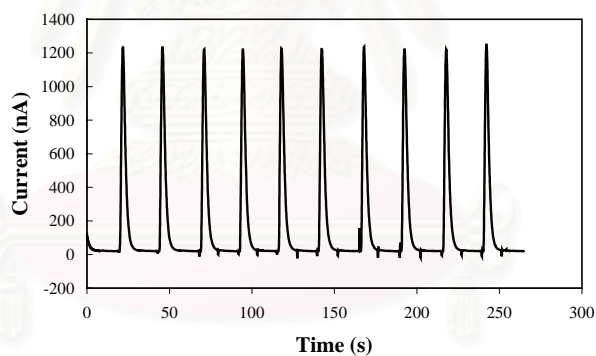


Figure 4.20 Diamond thin-film response to 10 20- $\mu$ L injections of (A) 10  $\mu$ M cysteine, (B) 50  $\mu$ M homocysteine and (C) 50  $\mu$ M 2-mercaptoethane sulfonic acid in 0.1 M carbonate buffer, pH 9.2. Flow rate 1.0 mL/min. Detection potential 0.55, 0.775 and 0.625, respectively.

The repeatability depended on the noise while an injection port was switched. A summary of repeatability of sulfur-containing compounds is shown in Table 4.4

Table 4.4 Peak variability of sulfur-containing compounds

|                                | Peak variability (%) |
|--------------------------------|----------------------|
| Cysteine                       | 2.56                 |
| Homocysteine                   | 6.35                 |
| 2-Mercaptoethane sulfonic acid | 3.66                 |

#### 4.5 Detection limit

The limit of detection was studied by examining various concentrations of sulfur-containing compounds from 50  $\mu$ M to 10 nM. The calibration curves of each sulfur-containing compound were obtained. The linear range was searched from calibration curve and trend line. The detection limit was defined by  $S/N > 3$ . It was found that, sulfur-containing compounds are polar molecules and can adsorb on the surface of tubing surface and injection port. When 0.1 M carbonate buffer pH 9.2 was injected as a blank, some of sulfur-containing compounds adsorbed on the surface of tubing were eluted through flow cell. Therefore, signals of sulfur impurities were obtained. Then the detection limit definition was the concentration of sulfur-containing compounds that had S/N ratio more than 3 and its signal was also more than the blank signal.

#### 4.5.1 Cysteine

Figure 4.21 shows FI results for five 20- $\mu$ L injections of 100 nM cysteine in 0.1 M carbonate buffer, pH 9.2. The flow rate of mobile phase was 1.0 mL/min. The detection potential was 0.55 V. The signal exhibits a faradaic response and a low background. The reproducibility of peak height and the minimal peak tailing are obtained. From the FIA data of various concentration of cysteine, a calibration curve plotted from concentration 50 nM to 50  $\mu$ M of cysteine was produced (Figure 4.22). The correlation coefficient of 0.9991 was received from this plot. The detection limit of cysteine was 50 nM.

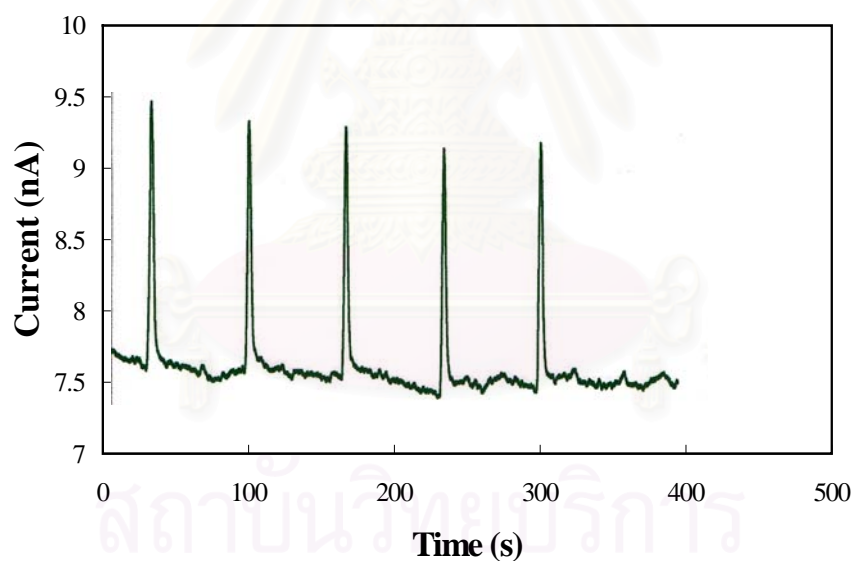


Figure 4.21 Diamond thin-film response to 5 20- $\mu$ L injections of 100 nM cysteine, in 0.1 M carbonate buffer, pH 9.2. Flow rate 1.0 mL/min. Detection potential 0.55 V.



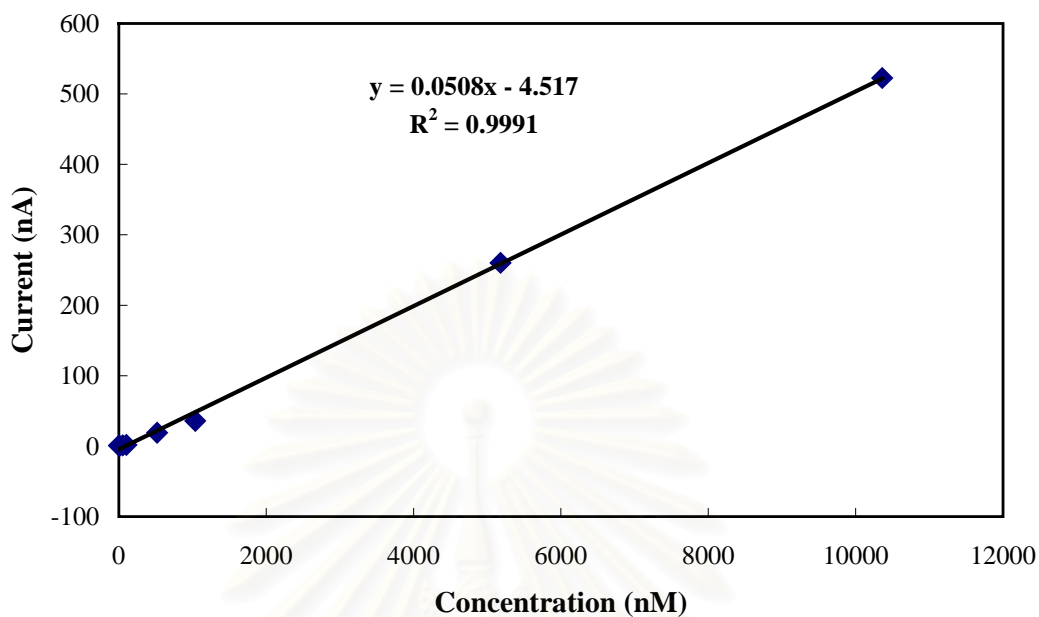


Figure 4.22 Calibration curve of cysteine in 0.1 M carbonate buffer, pH 9.2. Flow rate 1.0 mL/min. Detection potential 0.55 V.

#### 4.5.2 Homocysteine

Figure 4.23 shows the FI results for ten 20- $\mu$ L injections of 200 nM cysteine in 0.1 M carbonate buffer, pH 9.2. The flow rate of mobile phase was 1.0 mL/min. The detection potential was 0.775 V. The signal showed a high faradaic response and a low background. The reproducibility of peak height was good and the minimal peak tailing are observed for each concentration. From the examined data of various concentrations of homocysteine, a calibration curve was produced (Figure 4.24). A good calibration curve could not be produced because of the fluctuation of data from various concentrations. However, the data for each concentration

reproduced. Therefore the fluctuation of data may be caused by auto-oxidation or decomposition of the compound while the solution were diluted.

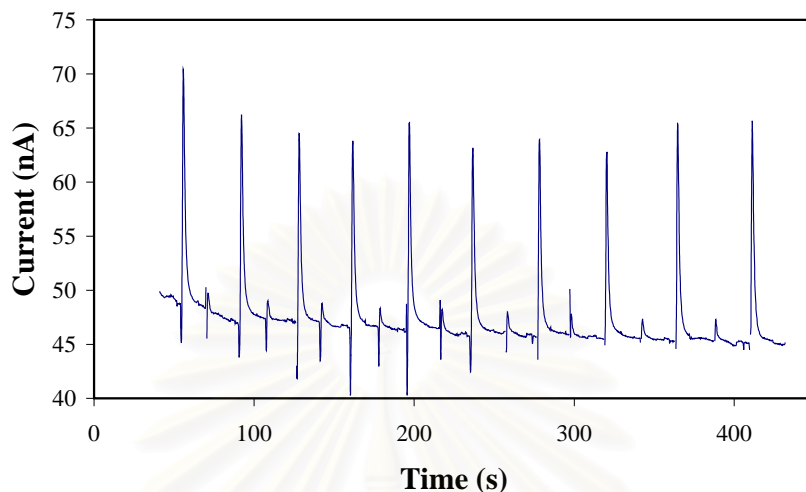


Figure 4.23 Diamond thin-film response to 10 20- $\mu$ L injections of 100 nM homocysteine, in 0.1 M carbonate buffer, pH 9.2. Flow rate 1.0 mL/min. Detection potential 0.775 V.

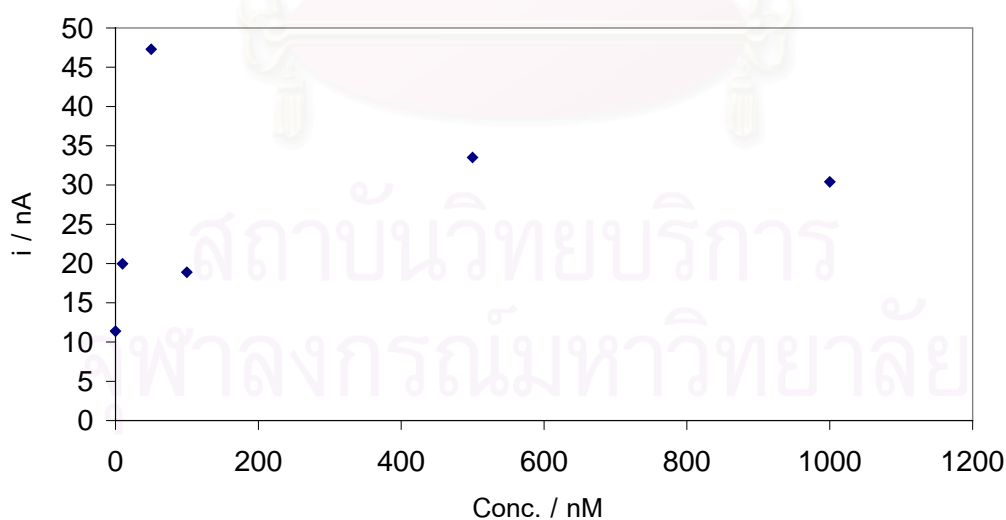


Figure 4.24 Calibration curve of homocysteine in 0.1 M carbonate buffer, pH 9.2. Flow rate 1.0 mL/min. Detection potential 0.775 V.

#### 4.5.3 2-Mercaptoethane sulfonic acid

Figure 4.25 shows FI results for five 20- $\mu$ L injections of 100 nM 2-mercaptoethane sulfonic acid in 0.1 M carbonate buffer, pH 9.2. The flow rate of mobile phase was 1.0 mL/min. The detection potential was 0.625 V. The signal exhibits a faradaic response and a low background. The reproducibility of peak height and the minimal peak tailing were obtained. The calibration curve was obtained from the FI data of various concentration of 2-mercaptoethane sulfonic acid (Figure 4.26). The correlation coefficient from this curve was 0.9999. The detection limit of 2-mercaptoethane sulfonic acid was 50 nM.

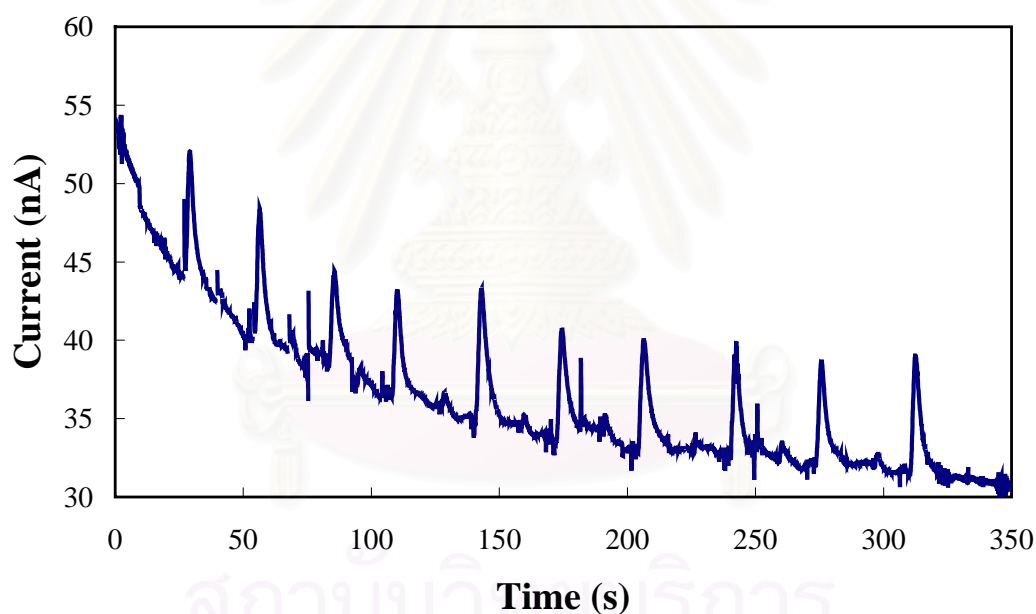


Figure 4.25 Diamond thin-film response to 10 20- $\mu$ L injections of 100 nM 2-mercaptoethane sulfonic acid, in 0.1 M carbonate buffer, pH 9.2. Flow rate 1.0 mL/min. Detection potential 0.625 V.

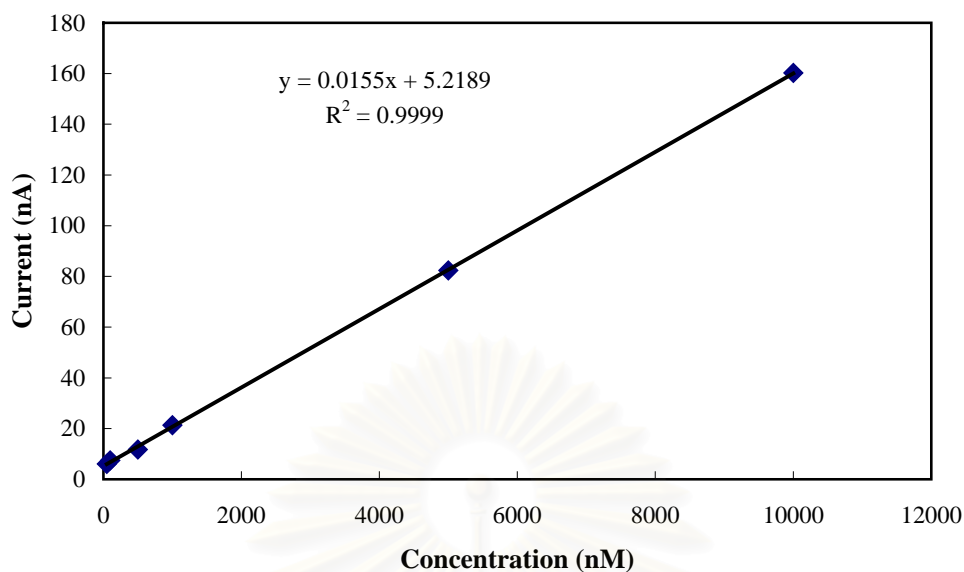


Figure 4.26 Calibration curve of 2-mercaptoethane sulfonic acid in 0.1 M carbonate buffer, pH 9.2. Flow rate 1.0 mL/min. Detection potential 0.625 V.

The summary of analytical data for flow injection analysis of sulfur-containing compound was shown in Table 4.5.

Table 4.5 The linear range, sensitivity, detection limit and peak variability of sulfur-containing compounds

|                                | Linear range     | Sensitivity<br>(nA/ $\mu$ M) | LOD<br>(nM) | % RSD |
|--------------------------------|------------------|------------------------------|-------------|-------|
| Cysteine                       | 50 nM-50 $\mu$ M | 50.9                         | 50          | 2.56  |
| Homocysteine                   | -                | -                            | -           | 6.35  |
| 2-Mercaptoethane sulfonic acid | 50 nM-10 $\mu$ M | 15.5                         | 50          | 3.66  |

#### 4.6 Comparison with the Other Flow Cell

The background hydrodynamic curve in 0.1 M carbonate buffer was studied, pH 9.2 with home-made flow cell. The FI results are shown in Figure 4.27. The signal showed a higher noise than the one from the BAS flow cell. The noise occurred from turbulent effects in the cell. The BAS flow cell has small inner inlet diameter (0.25 mm) while the inlet diameter of the home-made flow cell was 1.3 mm. The large inlet diameter introduced turbulence when the liquid collided with the surface of electrode. A salt-bridge was another cause of noise, the electrode transfer with the small salt-bridge was not good and the resistance of system was increased.

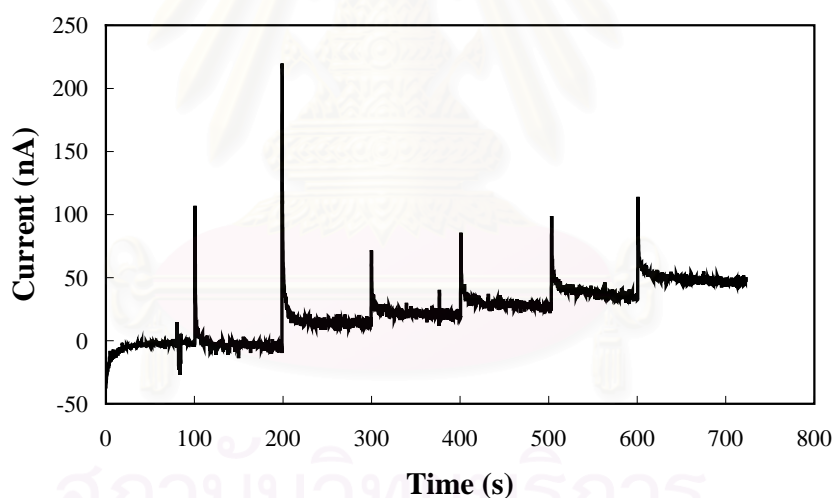


Figure 4.27 Signals of background hydrodynamic study of 0.1 M carbonate buffer, pH 9.2 using boron-doped diamond thin-film with home-made flow cell. Flow rate 1.0 mL/min. The sharply signal occurred from potential change.

Using the BAS flow cell and a boron-doped diamond thin-film electrode, it was found that 2-mercaptoethane sulfonic acid provided the most well-defined peak shape. It also found that 2-mercaptoethane sulfonic acid did not decompose during the time of preparation. Therefore, 2-mercaptoethane sulfonic acid was chosen to investigate the performance of the home-made flow cell. The hydrodynamic curve of 2-mercaptoethane sulfonic acid using the home-made flow cell is shown in Figure 4.28. Although this flow cell produced many noises, a hydrodynamic curve provided the same optimize potential as the one of the BAS flow cell (0.625 V).

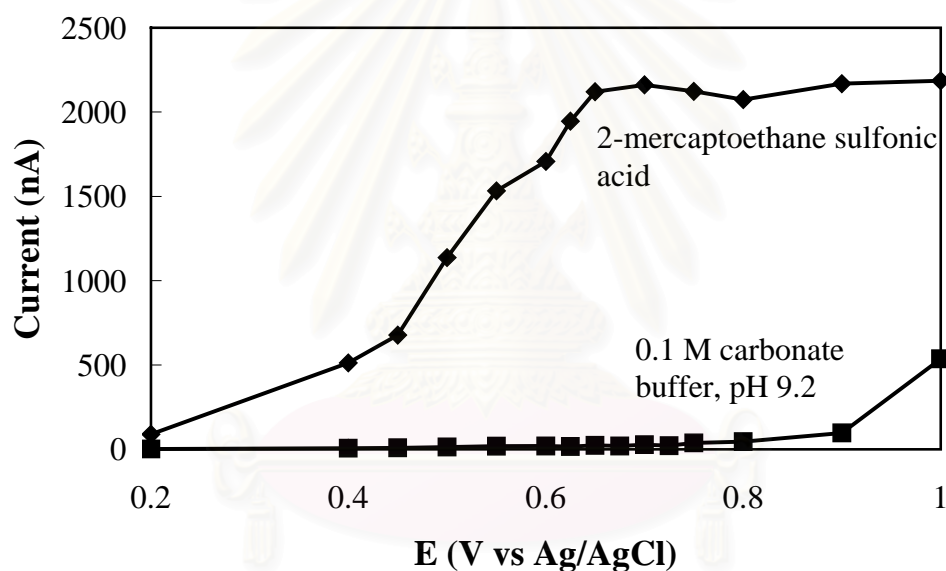


Figure 4.28 Background and 50  $\mu\text{M}$  2-mercaptoethane sulfonic acid hydrodynamic  $i$ - $E$  curves for boron-doped diamond thin-film electrode with home-made flow cell in 0.1 M carbonate buffer, pH 9.2. Flow rate 1.0 mL/min.

Figure 4.29 shows FI results for five 20- $\mu\text{L}$  injections of 10  $\mu\text{M}$  2-mercaptoethane sulfonic acid in 0.1 M carbonate buffer pH 9.2. The flow rate of mobile phase was 1.0 mL/min. The detection potential was 0.625 V. The minimal

peak tailing and the reproducibility of peak height were observed. From the FI data of various concentration of 2-mercaptoethane sulfonic acid, a calibration curve was produced (Figure 4.30). The correlation coefficient was 0.9928 from concentration 500 nM to 50  $\mu$ M of 2-mercaptoethane sulfonic acid. It indicated that the analytical data could be obtained from a boron-doped diamond thin-film electrode applied to flow injection system. The detection limit of 2-mercaptoethane sulfonic acid was 500 nM.

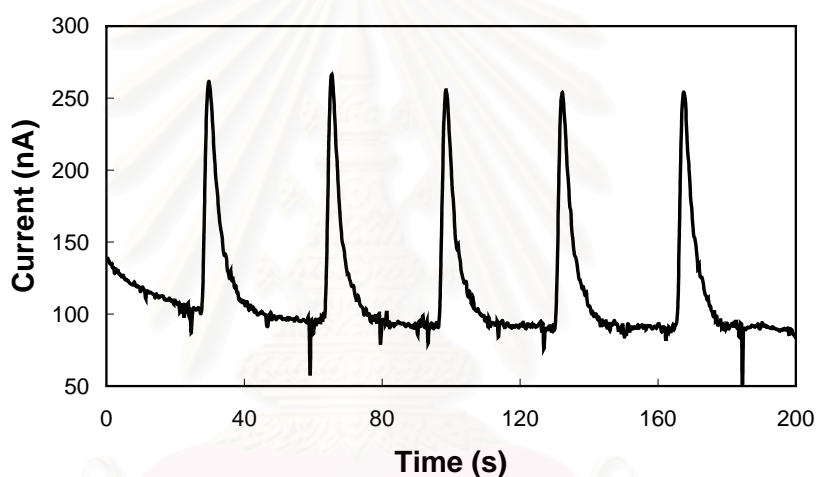


Figure 4.29 Diamond thin-film response to five 20- $\mu$ L injections of 10  $\mu$ M 2-mercaptoethane sulfonic acid for boron-doped diamond thin-film electrode with home-made flow cell in 0.1 M carbonate buffer, pH 9.2. Flow rate 1.0 mL/min. Detection potential 0.625 V.



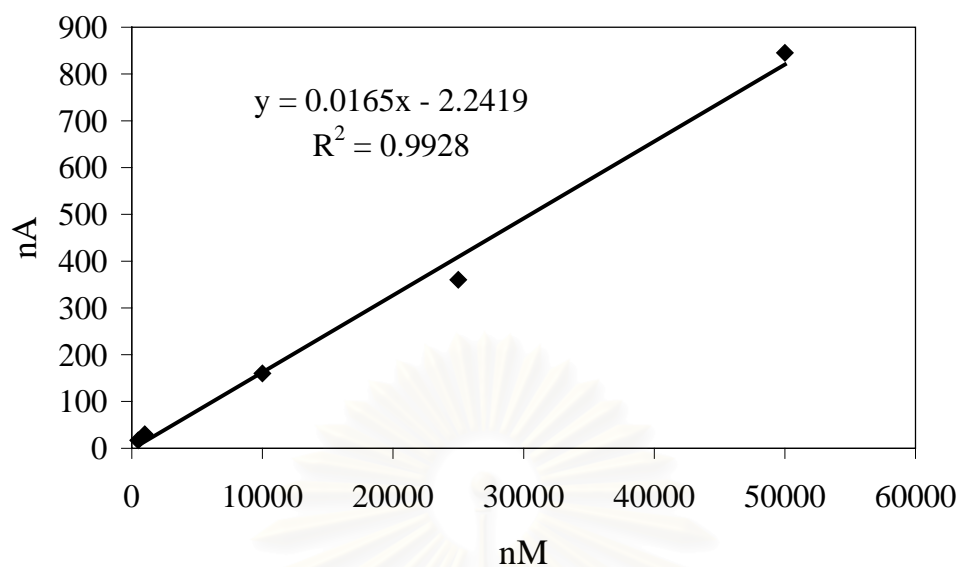


Figure 4.30 Calibration curve of 2-mercaptoethane sulfonic acid in 0.1 M carbonate buffer, pH 9.2 by flow injection analysis with home-made flow cell.

Table 4.6 shows the comparison of flow injection data of 2-mercaptoethane sulfonic acid from BAS flow cell and a home-made flow cell. Although a turbulent effect produced noise and high variability when using the home-made flow cell, the double-layer on electrode surface will decrease so the sensitivity of this cell was higher than that of the BAS flow cell.

Table 4.6 The linear range, sensitivity, detection limit and peak variability of sulfur-containing compounds

|                     | Linear range      | Sensitivity*  | Detection limit | % RSD |
|---------------------|-------------------|---------------|-----------------|-------|
|                     |                   | (nA/ $\mu$ M) | (nM)            |       |
| BAS flow cell       | 50 nM-10 $\mu$ M  | 15.5 $\pm$ 3  | 50              | 3.66  |
| Home-made flow cell | 500 nM-50 $\mu$ M | 16.5 $\pm$ 6  | 500             | 4.02  |

\* n=2

## CHAPTER V

### CONCLUSIONS AND SUGGESTION FOR FURTHER WORKS

#### 5.1 Conclusion

##### 5.1.1 The oxidation of sulfur-containing compounds

The oxidation of sulfur-containing compounds dissolved in aqueous media has been investigated using a boron-doped diamond thin-film and a glassy carbon electrodes with cyclic voltammetry. The boron-doped diamond thin-film electrode exhibited an analytical useful response for the sulfur-containing compounds. The results indicated that the boron-doped diamond was an excellent electrode for detecting sulfur-containing compounds. Peak shape of cyclic voltammograms received from the boron-doped diamond thin-film was better defined than the one from the glassy carbon electrode. A linear dynamic range of 1-2 order of magnitude and a detection limit of 0.5 mM were observed. It was also found that the oxidative product could cover the electrode surface and decreased the next scan signal. Flow injection analysis (FIA) was chosen to overcome this problem. The scan rate dependence indicated that the sulfur-containing compound products did not adsorb on the surface of diamond thin-film electrode.

##### 5.1.2 Flow injection analysis

The results of FIA from the BAS flow cell showed a good reproducibility. A linear dynamic range of cysteine and 2-mercaptoethane sulfonic acid of 4-5 order of magnitude and detection limit of 50.0 nM at a  $S/N = 3$  were observed for boron-doped diamond thin-film. The calibration curve of homocysteine can not be exhibited because of its auto-oxidation in a diluted solution.

### 5.1.3 A home-made flow cell

A home made flow cell provided well-defined signals for the sulfur-containing compounds. The current response was reproducible with the relative standard deviation of 4.02. However, signals from this cell showed a higher noise than those from the BAS flow cell. This noise could come from turbulent effects. A linear dynamic range of 2-mercaptoethane sulfonic acid of 3-4 order of magnitude and detection limit of 500 nM at a S/N = 3 were obtained for the boron-doped diamond thin-film.

## 5.2. Suggestion for further works

The study of sulfur-containing compound in real samples such as human blood serum is interesting. However, it has not been studied in this work yet because of a limitation of instrument and budget. Therefore, the separation and detection of these compounds by HPLC-EC should be tried for the further work.

For a development of the home-made flow cell, two weak points of it were size of the inlet and a salt-bridge. The inlet diameter should be decreased for the decreasing of turbulent effect. To reduce the resistance of the salt-bridge, making the small crossing area should be attempted.

## REFERENCES

1. H. C. Potgieter, J. B. Ubbink, S. Bissbort, M. J. Bester, and J. H. Spies. Anal. Biochem. 86 (1997):
2. L. Stryer. Biochemistry. 3rd. Ed. New York:Freeman, 1988.
3. P. J. Vanderburg and D. C. Jonhson. Analytical Chemistry 8 (1983):
4. G. S. Owens and W. R. LaCourse. Pulsed electrochemical detection of sulfur-containing compounds following microbore liquid chromatography. Current Sep. 3-4 (1996):82.
5. S. Zhang, W. Sun, Y. Xian, W. Zhang, L. Jin, K. Yamamota, S. Tao, and J. Jin. Multichannel amperometric detection system for liquid chromatography to assay thiols in human whole blood using the platinum microelectrodes chemically modified by copper tetraaminophthlocyanine. Anal. Chim. Acta. (1999):213.
6. M. Heyrovsky and S. Vavricka. Electrochemical reactivity of homocysteine at mercury electrode as compared with cysteine. Bioelectrochem. & Bioenerg. (1999):43.
7. N. D. Popavic and D. C. Johnson. Amperometric detection of biologically significant sulfur-containing compounds at Bi(V)-doped PbO<sub>2</sub> Film electrodes. Electroanalysis 13 (1999):934.
8. J. Xu, M. C. Granger, Q. Chen, J. W. Strojek, T. E. Lister, and G. M. Swain. Boron-Doped Diamond Thin-Film Electrodes. Anal. Chem. News and Features 19 (1997):591A.

9. J. Ruzicka and E. H. Hansen. Flow Injection Analysis. 2nd. Ed. New York:John Wiley &Son, 1988.
10. S. Jolley, M. Koppang, T. Jackson, and G. M. Swain. Flow Injection Analysis with Diamond Thin-Film Detectors. Anal. Chem. 20 (1997):4099.
11. J. Xu and G. M. Swain. Oxidation of Azide Anion at Boron-Doped Diamond Thin-Film Electrodes. Anal. Chem. 8 (1998):1502.
12. O. Chailapakul, E. Popa, H. Tai, D. A. Sarada, D. A. Tryk, and A. Fujishima. The electrooxidation of organic acids at boron-doped diamond electrodes. Electrochem. Commun. 2 (2000):422.
13. M. D. Koppang, M. Witek, J. Blau, and G. M. Swain. Electrochemical Oxidation of Polyamines at Diamond Thin-Film Electrodes. Anal. Chem. 6 (1999):1188.
14. A. J. Bard and L. R. Faulkner. Electrochemical Methods. 1st. Ed. New York:John Wiley & Sons, 1980.

## CURRICULUM VITAE

|                                |   |
|--------------------------------|---|
| <b>Name</b>                    | <b>Pakatip Aksharanandana</b>   |
| <b>Date and place of birth</b> | 25 March 1976, Rachaburi, THAILAND  |
| <b>Gender</b>                  | <b>Female</b>   |
| <b>Education:</b>              | <b>2000-1998 Chulalongkorn University,<br/>Master degree in Analytical chemistry</b>  |
|                                | 1997-1994 Chulalongkorn University, Bachelor of Science<br>(Second honor)   |
|                                | 1993-1991 Bodindecha (Singha Singhaseni) school, High<br>school   |
|                                | 1990-1988 Benchama Thep-uthit school, Petchburi,<br>Secondary school  |
|                                | 1987-1982 Aroonpradit school, Petchburi, Primary school   |
| <b>Honor and awards</b>        |   |
|                                | <ul style="list-style-type: none"><li>• Student of The development and promotion of science and technology talent project</li></ul> |

สถาบันวิทยบริการ  
จุฬาลงกรณ์มหาวิทยาลัย